JAMMER PLACEMENT ALGORITHMS FOR WIRELESS LOCALIZATION SYSTEMS

A THESIS SUBMITTED TO
THE GRADUATE SCHOOL OF ENGINEERING AND SCIENCE
OF BILKENT UNIVERSITY
IN PARTIAL FULFILLMENT OF THE REQUIREMENTS FOR
THE DEGREE OF
MASTER OF SCIENCE
IN
ELECTRICAL AND ELECTRONICS ENGINEERING

By
Mehmet Necip Kurt
July 2016

JAMMER PLACEMENT ALGORITHMS FOR WIRELESS LOCALIZATION SYSTEMS

By Mehmet Necip Kurt

July 2016

We certify that we have read this thesis and that in our opinion it is fully adequate, in scope and in quality, as a thesis for the degree of Master of Science.

Sinan Gezici (Advisor)

Orhan Arıkan

Berkan Dülek

Approved for the Graduate School of Engineering and Science:

Levent Onural
Director of the Graduate School

ABSTRACT

JAMMER PLACEMENT ALGORITHMS FOR WIRELESS LOCALIZATION SYSTEMS

Mehmet Necip Kurt
M.S. in Electrical and Electronics Engineering
Advisor: Sinan Gezici
July 2016

The optimal jammer placement problem is proposed and analyzed for wireless localization systems. In particular, the optimal location of a jammer node is obtained by maximizing the minimum of the Cramér-Rao lower bounds (CRLBs) for a number of target nodes under location related constraints for the jammer node. For scenarios with more than two target nodes, theoretical results are derived to specify conditions under which the jammer node is located as close to a certain target node as possible, or the optimal location of the jammer node is determined by two of the target nodes. Also, explicit expressions are provided for the optimal location of the jammer node in the presence of two target nodes. In addition, in the absence of distance constraints for the jammer node, it is proved, for scenarios with more than two target nodes, that the optimal jammer location lies on the convex hull formed by the locations of the target nodes and is determined by two or three of the target nodes, which have equalized CRLBs. Numerical examples are presented to provide illustrations of the theoretical results in different scenarios. Furthermore, an iterative algorithm is proposed for numerically determining the optimal jammer location. At each iteration of the algorithm, the jammer node is moved one step along a straight line with the purpose of increasing the CRLB(s) of the target node(s) with the minimum CRLB in the system. It is shown that the algorithm converges almost surely to the optimal jammer location under certain conditions for an infinitesimally small step size in the absence of location constraints for the jammer node. Simulations illustrate the effectiveness of the proposed algorithm in finding the optimal jammer location and its superiority in terms of the computational complexity compared to the exhaustive search over all feasible locations.

Keywords: Localization, jammer, Cramér-Rao lower bound, max-min.

ÖZET

TELSİZ KONUM BELİRLEME SİSTEMLERİ İÇİN KARIŞTIRICI YERLEŞTİRME ALGORİTMALARI

Mehmet Necip Kurt
Elektrik ve Elektronik Mühendisliği, Yüksek Lisans
Tez Danışmanı: Sinan Gezici
Temmuz 2016

Telsiz konum belirleme sistemleri için karıştırıcının en iyi şekilde yerleştirilmesi problemi önerilmekte ve çözümlenmektedir. Karıştırıcı düğümünün en iyi konumu, karıştırıcı düğümü için bazı konum kısıtlamaları gözetilerek, sistemdeki hedef düğümlerinin en düşük Cramér-Rao alt sınırını (CRLB) en yüksek seviyeye çıkaran nokta olarak elde edilmektedir. Sistemde ikiden fazla hedef düğümü olduğu durumlarda, karıştırıcı düğümünün belirli bir hedef düğümüne olabildiğince yakın olduğu veya en iyi karıştırıcı düğümü konumunun iki hedef düğümü tarafından belirlendiği koşulları belirten kuramsal sonuçlar çıkarılmaktadır. Ayrıca sistemde iki hedef düğümü olduğu durumlarda, en iyi karıştırıcı konumu için açık ifadeler sağlanmaktadır. Buna ek olarak, karıştırıcı düğümü için konum kısıtlamalarının olmadığı ve sistemde ikiden fazla hedef düğümü olduğu durumlarda, en iyi karıştırıcı düğümü konumunun birbirine eşit CRLB'ye sahip iki ya da üç hedef düğümünün konumları tarafından oluşturulan dışbükey zarf üzerinde olduğu ispat edilmektedir. Elde edilen kuramsal sonuçları farklı durumlarda açıklamak için sayısal örnekler sunulmaktadır. Ayrıca en iyi karıştırıcı konumunu sayısal olarak belirlemek için özyineli bir algoritma önerilmektedir. Algoritmanın her bir özyinelemesinde, karıştırıcı düğümü, sistemde o an için bulunan en küçük CRLB'ye sahip hedef düğümü veya düğümlerinin CRLB'lerini artırmak amacıyla düz bir doğru parçası üzerinde hareket ettirilmektedir. Karıştırıcı düğümü için konum kısıtlaması olmadığı durumlarda ve bazı koşullar altında, algoritmanın sonsuz küçük adım boyutu kullanılarak en iyi karıştırıcı düğümü konumuna hemen hemen kesin olarak yakınsadığı ispat edilmektedir. Benzetimler, önerilen algoritmanın en iyi karıştırıcı konumunu belirlemedeki etkinliğini ve hesaplama karmaşıklığı açısından bütün muhtemel konumlar üzerinde kapsamlı aramaya göre avantajını göstermektedir.

Anahtar sözcükler: Konum belirleme, karıştırıcı, Cramér-Rao alt sınırı, maks-min.

Acknowledgement

I would like to thank my advisor Assoc. Prof. Sinan Gezici for his guidance throughout my M.S. study. It was a great pleasure for me to work with him.

I thank my thesis commitee members Prof. Orhan Arıkan and Assoc. Prof. Berkan Dülek for their valuable efforts.

I thank all of my instructors in my life from primary school up to now for their valuable contributions on my personal and intellectual development.

I acknowledge that TÜBİTAK BİDEB 2210 Scholarship Program has financially supported me during my M.S. study.

I would like to express my deepest gratitude to my family. They are the most important and special part of my life. I would like to thank my parents, Hatice and Mahmut Kurt and my sisters Mine, Ayşe, and Merve for their support throughout my life.

Contents

List of Figures

List of Tables

Chapter 1

Introduction

Position information has a critical role for various location aware applications and services in current and next generation wireless systems [1, 2]. In the absence of GPS signals, e.g., due to lack of access to GPS satellites in some indoor environments, position information is commonly extracted from a network consisting of a number of anchor nodes at known locations via measurements of position related parameters such as time-of-arrival (TOA) or received signal strength (RSS) [2]. In such wireless localization networks, the aim is to achieve high localization accuracy, which is commonly defined in terms of the mean squared position error [3].

Jamming can degrade performance of wireless localization systems and can have significant effects in certain scenarios. Although jamming and anti-jamming approaches are investigated for GPS systems in various studies such as [4–6], effects of jamming on wireless localization networks have gathered little attention in the literature. Recently, a wireless localization network is investigated in the presence of jammer nodes, which aim to degrade the localization accuracy of the network, and the optimal power allocation strategies are proposed for the jammer nodes to maximize the average or the minimum Cramér-Rao lower bounds (CRLBs) of the target nodes [7]. The results provide guidelines for quantifying the effects of jamming in wireless localization systems [7].

The study in [7] assumes fixed locations for the jammer nodes and aims to perform optimal power allocation, which leads to convex (linear) optimization problems. In this thesis, the main purpose is to determine the optimal location of a jammer node in order to achieve the best jamming performance in a wireless localization network consisting of multiple target nodes. In particular, the optimal location of the jammer node is investigated to maximize the minimum of the CRLBs for the target nodes in a wireless localization network in the presence of constraints on the location of the jammer node. Although there exist some studies that investigate the jammer placement problem for communication systems, e.g., to prevent eavesdroppers [8] or to jam wireless mesh networks [9], the optimal jammer placement problem has not been considered for wireless localization networks in the literature.

1.1 Literature Survey on Node Placement

Optimal node placement has been studied intensely for wireless sensor networks (WSNs) in the last decade, and various objectives have been considered for placement of sensor nodes. For example, in [10] and [11], the aim is to provide complete coverage of the WSN area with the minimum number of sensor nodes. In [12], the aim is to maximize the lifetime of the network via distance based placement whereas the resilience of the network to single node failures is the main objective in [13]. In another study, powerful relay nodes are placed together with sensor nodes in order to increase the lifetime of the network [14].

Placement of jammer nodes in wireless networks can be performed for various purposes [15]. While the aim of jammer placement is generally to create disruptive effects on the network operation, different objectives are also considered in the literature. In [16], the aim is to divide network into subparts and to prevent the network traffic between those subparts via jamming. In [9], the main objective is to destroy the communication links in the network in the worst possible way by placing jammer nodes efficiently. On the other hand, in [8], the purpose of using jammer nodes is to protect the network from eavesdroppers, and the

function of jammer nodes is to reduce signal quality below a level such that no illegitimate receiver can reach the network data. During this protection, signal quality must be kept above a certain level for other devices so that the actual network operation is not prevented. Based on these two main criteria, the optimal placement of jammer nodes are performed in [8].

Against jamming attacks, various anti-jamming techniques have also been developed [17–23]. Some studies such as [20] focus on finding positions of jamming devices for taking security actions against them; e.g., physically destroying them or changing the routing protocol, in order not to traverse the jammed region [20]. Another technique is to rearrange the positions of the nodes in the network after each attack in order to mitigate the effects of jamming [23]. In addition, [15] employs a game theoretic approach, in which the attacker tries to maximize the damage on the network activity while the aim of the defender is to secure the multi-hop multi-channel network. Actions available to the attacker are related to choosing the positions of jammer nodes and the channel hopping strategy while the action of the defender is based on choosing the channel hopping strategy.

In the literature, there also exist some practical heuristic approaches for node placement. In case of jamming, placing jammer nodes close to source and destination nodes, at the critical transshipment points of the network, or where sensor nodes are dense are among such approaches [9]. By evaluating efficiency of different jammer locations, these heuristic approaches can be analyzed and compared for various scenarios. In some studies such as [8], the best jammer location is chosen among finitely many predetermined locations. The motivation behind this method is that it is not always possible to place jammer nodes at desired locations due to topological limitations, risk of visual detection by enemies, or tight security measurements [9]. In addition, for both jammer and sensor node placement, the grid-based approach is widely employed. In this approach, the continuous sensor field is divided into equal-area grid cells and the best location is determined via evaluation over finite set of points. As the grid size is reduced, performance of node placement improves in general; however, the required computational effort to find the best location increases as well. In [9], based on the grid-based approach, it is shown that the most disruptive effect on the network

occurs when jammer nodes are placed close to source and destination nodes. Similarly, in [15], it is stated that the optimal solution for jammer nodes is to jam the network flow concentrated near source and destination nodes.

Placement of anchor nodes has been studied for wireless localization systems, in which the aim is to perform optimal deployment of anchor nodes for improving localization accuracy of target nodes in the system [24–27]. For example, in [25], placement of anchor nodes is performed in order to minimize the CRLB in an RSS based localization system. It is stated that anchor nodes should be placed at the edges of the network area. On the other hand, the authors in [27] employ an optimization method based on the integer-coded genetic algorithm for optimizing the average localization error and the signal coverage estimate. In [26], it is stated that no three anchor nodes should be placed on a straight line.

1.2 Contributions

Although placement of anchor nodes is considered for wireless localization systems (e.g., [24–27]) and placement of jammer nodes is studied for communication systems (e.g., [8, 9, 16]), there exist no studies that investigate the problem of optimal jammer placement in wireless localization systems. In this thesis, the optimal jammer placement problem is proposed and analyzed for wireless localization systems [28]. In particular, the minimum of the CRLBs of the target nodes is considered as the objective function (to guarantee that all the target nodes have localization accuracy bounded by a certain limit) and constraints are imposed on distances between the jammer node and target nodes. In addition to the generic formulation, which leads to a non-convex problem, various special cases are investigated and theoretical results are presented to characterize the optimal solution. Especially, the scenario with two target nodes and the scenario with more than two target nodes and in the absence of distance constraints are investigated in detail. Various numerical examples are presented to verify and explain the theoretical results. In addition to the theoretical results, a numerical algorithm is proposed to determine the optimal jammer location. It is shown

that the proposed algorithm converges to the optimal jammer location under some conditions. Simulations illustrate that the algorithm is accurate to find the optimal jammer location and effective to reduce the computational burden compared to the grid-based exhaustive search algorithm. The main contributions of this thesis can be summarized as follows:

- The optimal jammer placement problem in a wireless localization system is proposed.
- In the presence of more than two target nodes, conditions are derived to specify scenarios in which the optimal jammer location is as close to a certain target node as possible (Proposition 1) or the jammer node is located on the straight line that connects two target nodes (Proposition 2). In addition, for the case of two target nodes, the optimal location of the jammer node is specified explicitly (Proposition 3).
- In the absence of distance constraints for the jammer node, it is proved, for scenarios with more than two target nodes, that the optimal location of the jammer node lies on the convex hull formed by the locations of the target nodes (Proposition 4), where the projection theorem is utilized for specifying the location of the jammer node.
- For scenarios with three target nodes and in the absence of distance constraints, it is shown that the optimal jammer location equalizes the CRLBs of either all the target nodes or two of the target nodes, which correspond to cases in which the jammer node lies on the interior or on the boundary of the triangle formed by the target nodes, respectively (Propositions 5 and 6-(a)). In addition, a necessary and sufficient condition is presented for the optimal jammer location to be on the interior or the boundary of that triangle (Proposition 6-(b)).
- In the absence of distance constraints for the jammer node and in the presence of more than three target nodes, it is proved that the optimal jammer location is determined by two or three of the target nodes (Proposition 7).

- A numerical algorithm is proposed to determine the optimal jammer location and it is proved that the optimal location is specified almost surely for an infinitesimally small step size in the absence of distance constraints under certain conditions (Proposition 8).

The main motivations behind the study of the optimal jammer placement problem for wireless localization are related to performing efficient jamming of a wireless localization system (e.g., of an enemy) to degrade localization accuracy, and presenting theoretical results on optimal jamming performance, which can be useful for providing guidelines for developing anti-jamming techniques (see Chapter 8).

Chapter 2

System Model

Consider a wireless localization network in a two-dimensional space consisting of N_A anchor nodes and N_T target nodes located at $\boldsymbol{y}_i \in \mathbb{R}^2$, $i = 1, \ldots, N_A$ and $\boldsymbol{x}_i \in \mathbb{R}^2$, $i = 1, \ldots, N_T$, respectively. It is assumed that $\boldsymbol{x}_i$'s ($\boldsymbol{y}_i$'s) are all distinct. The target nodes are assumed to estimate their locations based on received signals from the anchor nodes, which have known locations; i.e., self-positioning is considered [3]. In addition to the target and anchor nodes, there exists a jammer node at location $\boldsymbol{z} \in \mathbb{R}^2$, which aims to degrade the localization performance of the network. The jammer node is assumed to transmit zero-mean Gaussian noise, as commonly employed in the literature [9, 29–31].

In this thesis, non-cooperative localization is studied, where target nodes receive signals only from anchor nodes (i.e., not from other target nodes) for localization purposes. Also, the connectivity sets are defined as $\mathcal{A}_i \triangleq \{j \in \{1, \ldots, N_A\} \mid \text{anchor node } j \text{ is connected to target node } i\}$ for $i \in \{1, \ldots, N_T\}$. Then, the received signal at target node i coming from anchor node j is expressed as [7]

$$r_{ij}(t) = \sum_{k=1}^{L_{ij}} \alpha_{ij}^k s_j(t - \tau_{ij}^k) + \gamma_{ij}\sqrt{P_J}\, v_{ij}(t) + n_{ij}(t) \tag{2.1}$$

for $t \in [0, T_{\text{obs}}]$, $i \in \{1, \ldots, N_T\}$, and $j \in \mathcal{A}_i$, where T_{obs} is the observation time, α_{ij}^k and τ_{ij}^k represent, respectively, the amplitude and delay of the kth multipath

component between anchor node j and target node i, L_{ij} is the number of paths between target node i and anchor node j, P_J is the transmit power of the jammer node, and γ_{ij} denotes the channel coefficient between target node i and the jammer node during the reception of the signal from anchor node j. The transmit signal $s_j(t)$ is known, and the measurement noise $n_{ij}(t)$ and the jammer noise $\sqrt{P_J}\, v_{ij}(t)$ are assumed to be independent zero-mean white Gaussian random processes[1], where the spectral density level of $n_{ij}(t)$ is $N_0/2$ and that of $v_{ij}(t)$ is equal to one [7]. Also, for each $i \in \{1, \ldots, N_T\}$, $n_{ij}(t)$'s ($v_{ij}(t)$'s) are assumed to be independent for $j \in \mathcal{A}_i$.[2] The delay τ_{ij}^k is expressed as

$$\tau_{ij}^k = \left(\|\boldsymbol{y}_j - \boldsymbol{x}_i\| + b_{ij}^k \right) / c \tag{2.2}$$

with $b_{ij}^k \geq 0$ representing a range bias and c being the speed of propagation. Set $\mathcal{A}_i$ is partitioned as follows: $\mathcal{A}_i \triangleq \mathcal{A}_i^L \cup \mathcal{A}_i^{NL}$, where $\mathcal{A}_i^L$ and $\mathcal{A}_i^{NL}$ denote the sets of anchor nodes with line-of-sight (LOS) and non-line-of-sight (NLOS) connections to target node i, respectively.

It is noted from (2.1) that a constant jamming attack is considered in this study, where the jammer node constantly emits white Gaussian noise [33, 34]. This model is well-suited for scenarios in which the jammer node has the ability to transmit noise only, or does not know the ranging signals employed between the anchor and target nodes. In such scenarios, the jammer node can constantly transmit Gaussian noise for efficient jamming as the Gaussian distribution corresponds to the worst-case scenario among all possible noise distributions according to some criteria such as minimizing the mutual information and maximizing the mean-squared error [35–37].

Remark 1: In practical wireless localization systems, multiple access techniques, such as time division multiple access or frequency division multiple access,

[1]Even though it is theoretically possible to mitigate the effects of zero-mean white Gaussian noise by repeating measurements, the observation interval (the number of measurements) cannot be increased arbitrarily in practical localization systems since the location of a target node should approximately be constant during the observation interval. Also, increasing the observation interval for localization can lead to data rate reduction in systems that perform both localization and data transmission. When multiple independent measurements are taken, the λ_{ij} term in (3.6) can be scaled by the number of measurements.

[2]The transmitted signals, $s_j(t)$'s, are assumed to be orthogonal [32] (cf. Remark 1).

are employed so that the signal from each anchor node can be observed by each target node without any interference from the other anchor nodes, as stated in (2.1) [32]. Therefore, for each target node, the received signals related to different anchor nodes contain jamming signals that correspond to different time intervals or frequency bands; hence, for each i, $v_{ij}(t)$ for $j \in \mathcal{A}_i$ can be modeled as independent.

Chapter 3

CRLBs for Localization of Target Nodes

Regarding target node i, the following vector consisting of the bias terms in the LOS and NLOS cases is defined [38]:

$$\boldsymbol{b}_{ij} = \begin{cases} \left[b_{ij}^{2} \dots b_{ij}^{L_{ij}}\right]^{T}, & \text{if } j \in \mathcal{A}_i^{L} \\ \left[b_{ij}^{1} \dots b_{ij}^{L_{ij}}\right]^{T}, & \text{if } j \in \mathcal{A}_i^{NL} \end{cases}. \tag{3.1}$$

From (3.1), the unknown parameters related to target node i are defined as follows [39].

$$\boldsymbol{\theta}_i \triangleq \left[\boldsymbol{x}_i^T \ \boldsymbol{b}_{i\mathcal{A}_i(1)}^T \ \cdots \ \boldsymbol{b}_{i\mathcal{A}_i(|\mathcal{A}_i|)}^T \ \boldsymbol{\alpha}_{i\mathcal{A}_i(1)}^T \ \cdots \ \boldsymbol{\alpha}_{i\mathcal{A}_i(|\mathcal{A}_i|)}^T\right]^T \tag{3.2}$$

where $\mathcal{A}_i(j)$ denotes the jth element of set $\mathcal{A}_i$, $|\mathcal{A}_i|$ represents the number of elements in $\mathcal{A}_i$, and $\boldsymbol{\alpha}_{ij} = \left[\alpha_{ij}^{1} \cdots \alpha_{ij}^{L_{ij}}\right]^T$. The total noise level is assumed to be known by each target node.

The CRLB for location estimation is expressed as [39]

$$\mathbb{E}\left\{\|\hat{\boldsymbol{x}}_i - \boldsymbol{x}_i\|^2\right\} \geq \mathrm{tr}\left\{\left[\boldsymbol{F}_i^{-1}\right]_{2\times 2}\right\} \tag{3.3}$$

where $\hat{\boldsymbol{x}}_i$ represents an unbiased estimate of the location of target node i, tr denotes the trace operator, and $\boldsymbol{F}_i$ is the Fisher information matrix for vector $\boldsymbol{\theta}_i$.

Based on the steps in [39], $\left[\boldsymbol{F}_i^{-1}\right]_{2\times 2}$ in (3.3) can be stated as

$$\left[\boldsymbol{F}_i^{-1}\right]_{2\times 2} = \boldsymbol{J}_i(\boldsymbol{x}_i, P_J)^{-1} \tag{3.4}$$

where the equivalent Fisher information matrix $\boldsymbol{J}_i(\boldsymbol{x}_i, P_J)$ in the absence of prior information about the location of the target node is expressed as (see Theorem 1 in [39] for the derivations)

$$\boldsymbol{J}_i(\boldsymbol{x}_i, P_J) = \sum_{j\in\mathcal{A}_i^L} \frac{\lambda_{ij}}{N_0/2 + P_J|\gamma_{ij}|^2}\, \boldsymbol{\phi}_{ij}\boldsymbol{\phi}_{ij}^T \tag{3.5}$$

with

$$\lambda_{ij} \triangleq \frac{4\pi^2\beta_j^2|\alpha_{ij}^1|^2 \int_{-\infty}^{\infty}|S_j(f)|^2 df}{c^2}(1-\xi_{ij})\,, \tag{3.6}$$

$$\boldsymbol{\phi}_{ij} \triangleq \left[\cos\varphi_{ij} \;\; \sin\varphi_{ij}\right]^T. \tag{3.7}$$

In (3.6), β_j denotes the effective bandwidth, and is given by $\beta_j^2 = \int_{-\infty}^{\infty} f^2|S_j(f)|^2 df \big/ \int_{-\infty}^{\infty}|S_j(f)|^2\, df$, with $S_j(f)$ representing the Fourier transform of $s_j(t)$, and the path-overlap coefficient ξ_{ij} is a non-negative number between zero and one, that is, $0 \le \xi_{ij} \le 1$ [40]. In addition, φ_{ij} in (3.7) denotes the angle between target node i and anchor node j.

From (3.3) and (3.4), the CRLB for target node i can be expressed as follows:

$$\text{CRLB}_i = \text{tr}\left\{\boldsymbol{J}_i(\boldsymbol{x}_i, P_J)^{-1}\right\} \tag{3.8}$$

where $\boldsymbol{J}_i(\boldsymbol{x}_i, P_J)$ is as in (3.5).

Remark 2: Even though the jammer noise received at different target nodes can be correlated in some cases, this does not have any effects on the formulation of the CRLB for each target node since the CRLB for a target node depends only on the signals received by that target node (cf. (3.5) and (3.8)). In other words, since each target node is performing estimation of its own location, the jamming signals that affect the signals received by other target nodes are irrelevant for that target node.

Chapter 4

Optimal Jammer Placement

4.1 Generic Formulation and Analysis

The aim is to determine the optimal location for the jammer node in order to increase the CRLBs of all the target nodes as much as possible. The CRLB is considered as a performance metric since it bounds the localization performance of a target node in terms of the mean-squared error [32, 41, 42]. In particular, the minimum of the CRLBs of the target nodes is considered as the objective function to guarantee that all the target nodes have localization accuracy bounded by a certain limit. The proposed problem formulation is expressed, based on (3.8), as follows:

$$\begin{aligned} &\underset{\boldsymbol{z}}{\text{maximize}} \ \min_{i\in\{1,\ldots,N_T\}} \ \text{tr}\left\{\boldsymbol{J}_i(\boldsymbol{x}_i, P_J)^{-1}\right\} \\ &\text{subject to } \|\boldsymbol{z}-\boldsymbol{x}_i\| \geq \varepsilon \ , \quad i=1,\ldots,N_T \end{aligned} \tag{4.1}$$

where $\varepsilon > 0$ denotes the lower limit for the distance between a target node and the jammer node, which is incorporated into the formulation since it may not be possible for the jammer node to get very close to target nodes in practical jamming scenarios (e.g., the jammer node may need to hide) [9].

Similarly to [32] and [43], the channel power gain between the jammer node

and the ith target node is modeled as

$$|\gamma_{ij}|^2 = \tilde{K}_i \left(\frac{d_0}{\|\boldsymbol{z} - \boldsymbol{x}_i\|} \right)^{\nu} , \tag{4.2}$$

for $\|\boldsymbol{z} - \boldsymbol{x}_i\| > d_0$, where d_0 is the reference distance for the antenna far-field, ν is the path-loss exponent (commonly between 2 and 4), and $\tilde{K}_i$ is a unitless constant that depends on antenna characteristics and average channel attenuation [44]. It is assumed that $\tilde{K}_i$'s, d_0, ν, and ε are known, and that $\varepsilon > d_0$. (Also, the channel power gain between the jammer node and the ith target node is assumed to be constant during the reception of the signals from the anchor nodes.) From (4.2), the CRLB in (3.8) can be stated, based on (3.5), as follows:

$$\text{CRLB}_i = \text{tr}\left\{ \boldsymbol{J}_i(\boldsymbol{x}_i, P_J)^{-1} \right\} = R_i \left(\frac{K_i P_J}{\|\boldsymbol{z} - \boldsymbol{x}_i\|^{\nu}} + \frac{N_0}{2} \right) \tag{4.3}$$

where $K_i \triangleq \tilde{K}_i (d_0)^{\nu}$ and

$$R_i \triangleq \text{tr}\left\{ \left[\sum_{j \in \mathcal{A}_i^L} \lambda_{ij} \boldsymbol{\phi}_{ij} \boldsymbol{\phi}_{ij}^T \right]^{-1} \right\} . \tag{4.4}$$

Then, the optimization problem in (4.1) can be expressed, via (4.3), as follows:[1]

$$\begin{aligned} &\underset{\boldsymbol{z}}{\text{maximize}} \ \min_{i \in \{1,\ldots,N_T\}} R_i \left(\frac{K_i P_J}{\|\boldsymbol{z} - \boldsymbol{x}_i\|^{\nu}} + \frac{N_0}{2} \right) \\ &\text{subject to } \|\boldsymbol{z} - \boldsymbol{x}_i\| \geq \varepsilon \ , \quad i = 1, \ldots, N_T \end{aligned} \tag{4.5}$$

Since the jammer node is assumed to know the localization related parameters in this formulation, a performance benchmark is provided for the jamming of wireless localization systems, which corresponds to the best achievable performance for the jammer node and the worst-case scenario for the wireless localization network. Hence, based on the results in this study, a wireless localization network can

[1]The jammer node is assumed to know the localization related parameters so that it can solve the optimization problem in (4.5). Although this information may not completely be available to the jammer node in practical scenarios, this assumption is made for two purposes: (i) to obtain initial results which can form a basis for further studies on the problem of optimal jammer placement in wireless localization systems, (ii) to derive theoretical limits on the best achievable performance of the jammer node (if the jammer node is smart and can learn all the related parameters, the localization accuracy provided in this study is achieved; otherwise, the localization accuracy is bounded by the provided results).

specify the maximum amount of performance degradation that can be caused by a jammer node and take certain precautions accordingly (see Section 8).

The problem in (4.5) is non-convex; hence, convex optimization tools cannot be employed to obtain the optimal location of the jammer node. Therefore, an exhaustive search over the feasible locations for the jammer node may be required in general. However, some theoretical results are obtained in the following in order to simplify the optimization problem in (4.5) under various conditions.

Proposition 1: *If there exists a target node, say the ℓth one, that satisfies the following inequality,*

$$R_\ell\left(\frac{K_\ell P_J}{\varepsilon^\nu}+\frac{N_0}{2}\right) \leq \min_{\substack{i\in\{1,\ldots,N_T\}\\ i\neq\ell}} R_i\left(\frac{K_i P_J}{(\|\boldsymbol{x}_i-\boldsymbol{x}_\ell\|+\varepsilon)^\nu}+\frac{N_0}{2}\right) \tag{4.6}$$

and if set $\{\boldsymbol{z} : \|\boldsymbol{z}-\boldsymbol{x}_\ell\|=\varepsilon \ \&\ \|\boldsymbol{z}-\boldsymbol{x}_i\|\geq\varepsilon,\ i=1,\ldots,\ell-1,\ell+1,\ldots,N_T\}$ is non-empty, then the solution of (4.5), denoted by $\boldsymbol{z}^{\rm opt}$, satisfies $\|\boldsymbol{z}^{\rm opt}-\boldsymbol{x}_\ell\|=\varepsilon$; that is, the jammer node is placed at a distance of ε from the ℓth target node.

Proof. See Appendix A.1. □

Proposition 1 presents a scenario in which the jammer node must be as close to a certain target node (denoted by target node ℓ in the proposition) as possible in order to maximize the minimum of the CRLBs of the target nodes. In this scenario, the feasible set for the jammer location is significantly reduced, which simplifies the search space for the optimization problem in (4.5).

In order to specify another scenario in which the solution of (4.5) can be obtained in a simplified manner, consider the optimization problem in (4.5) in the presence of two target nodes ℓ_1 and ℓ_2 only; that is,

$$\begin{aligned} &\underset{\boldsymbol{z}}{\text{maximize}} \ \min_{i\in\{\ell_1,\ell_2\}} R_i\left(\frac{K_i P_J}{\|\boldsymbol{z}-\boldsymbol{x}_i\|^\nu}+\frac{N_0}{2}\right) \\ &\text{subject to } \|\boldsymbol{z}-\boldsymbol{x}_{\ell_1}\|\geq\varepsilon\,,\ \|\boldsymbol{z}-\boldsymbol{x}_{\ell_2}\|\geq\varepsilon \end{aligned} \tag{4.7}$$

where $\ell_1,\ell_2\in\{1,\ldots,N_T\}$ and $\ell_1\neq\ell_2$. Let $\boldsymbol{z}^{\rm opt}_{\ell_1,\ell_2}$ and $\mathrm{CRLB}_{\ell_1,\ell_2}$ denote the optimizer and the optimal value of (4.7), respectively. (In the next section, the

solution in the presence of two target nodes is investigated in detail.) Then, the following proposition characterizes the solution of (4.5) under certain conditions.

Proposition 2: *Let* $\mathrm{CRLB}_{k,i}$ *be the minimum of* $\mathrm{CRLB}_{\ell_1,\ell_2}$ *for* $\ell_1, \ell_2 \in \{1, \ldots, N_T\}$ *and* $\ell_1 \neq \ell_2$*, and let* $\boldsymbol{z}_{k,i}^{\mathrm{opt}}$ *denote the corresponding jammer location (i.e., the optimizer of* (4.7) *for* $\ell_1 = k$ *and* $\ell_2 = i$*). Then, an optimal jammer location obtained from* (4.5) *is equal to* $\boldsymbol{z}_{k,i}^{\mathrm{opt}}$ *if* $\boldsymbol{z}_{k,i}^{\mathrm{opt}}$ *is an element of set* $\left\{\boldsymbol{z} : \|\boldsymbol{z} - \boldsymbol{x}_m\| \geq \varepsilon,\, m \in \{1, \ldots, N_T\} \setminus \{k, i\}\right\}$ *and*

$$R_m \left(\frac{K_m P_J}{\|\boldsymbol{z}_{k,i}^{\mathrm{opt}} - \boldsymbol{x}_m\|^{\nu}} + \frac{N_0}{2} \right) \geq \mathrm{CRLB}_{k,i} \tag{4.8}$$

for $m \in \{1, \ldots, N_T\} \setminus \{k, i\}$.

Proof. From (4.5) and (4.7), it is noted that $\mathrm{CRLB}_{k,i}$, defined in the proposition, provides an upper bound for the problem in (4.5). If the conditions in (4.8) are satisfied, the objective function in (4.5) becomes equal to the upper bound, $\mathrm{CRLB}_{k,i}$, for $\boldsymbol{z} = \boldsymbol{z}_{k,i}^{\mathrm{opt}}$. Therefore, if $\boldsymbol{z}_{k,i}^{\mathrm{opt}}$ satisfies the distance constraints (i.e., if it is feasible for (4.5)), it becomes the solution of (4.5). □

Proposition 2 specifies a scenario in which the optimal jammer location is mainly determined by two of the target nodes since the others have larger CRLBs when the jammer node is placed at the optimal location according to those two jammer nodes only. In such a scenario, the optimal jammer location can be found easily, as the solution of (4.7) is simple to obtain (in comparison to (4.5)), which is investigated in the following section.

4.2 Special Case: Two Target Nodes

In the case of two target nodes, the solution of (4.5) can easily be obtained based on the following result.

Proposition 3: *For the case of two target nodes (i.e.,* $N_T = 2$*), the solution* $\boldsymbol{z}^{\mathrm{opt}}$ *of* (4.5) *satisfies one of the following conditions:*

(i) *if* $\|\boldsymbol{x}_1 - \boldsymbol{x}_2\| < 2\,\varepsilon$, *then* $\|\boldsymbol{z}^{\text{opt}} - \boldsymbol{x}_1\| = \|\boldsymbol{z}^{\text{opt}} - \boldsymbol{x}_2\| = \varepsilon$.

(ii) *otherwise,*

(a) *if* $R_1\left(\frac{K_1 P_J}{\varepsilon^\nu} + \frac{N_0}{2}\right) \leq R_2\left(\frac{K_2 P_J}{(\|\boldsymbol{x}_1 - \boldsymbol{x}_2\| - \varepsilon)^\nu} + \frac{N_0}{2}\right)$, *then* $\|\boldsymbol{z}^{\text{opt}} - \boldsymbol{x}_1\| = \varepsilon$ *and* $\|\boldsymbol{z}^{\text{opt}} - \boldsymbol{x}_2\| = \|\boldsymbol{x}_1 - \boldsymbol{x}_2\| - \varepsilon$.

(b) *if* $R_2\left(\frac{K_2 P_J}{\varepsilon^\nu} + \frac{N_0}{2}\right) \leq R_1\left(\frac{K_1 P_J}{(\|\boldsymbol{x}_1 - \boldsymbol{x}_2\| - \varepsilon)^\nu} + \frac{N_0}{2}\right)$, *then* $\|\boldsymbol{z}^{\text{opt}} - \boldsymbol{x}_1\| = \|\boldsymbol{x}_1 - \boldsymbol{x}_2\| - \varepsilon$ *and* $\|\boldsymbol{z}^{\text{opt}} - \boldsymbol{x}_2\| = \varepsilon$.

(c) *otherwise,* $\|\boldsymbol{z}^{\text{opt}} - \boldsymbol{x}_1\| = d^*$ *and* $\|\boldsymbol{z}^{\text{opt}} - \boldsymbol{x}_2\| = \|\boldsymbol{x}_1 - \boldsymbol{x}_2\| - d^*$, *where* d^* *is the unique solution of the following equation over* $d \in (\varepsilon,\, \|\boldsymbol{x}_1 - \boldsymbol{x}_2\| - \varepsilon)$.

$$R_1\left(\frac{K_1 P_J}{d^\nu} + \frac{N_0}{2}\right) = R_2\left(\frac{K_2 P_J}{(\|\boldsymbol{x}_1 - \boldsymbol{x}_2\| - d)^\nu} + \frac{N_0}{2}\right) \tag{4.9}$$

Proof. See Appendix A.2. □

Based on Proposition 3, the optimal location of the jammer node can be specified for $N_T = 2$ as follows: If the distance between the target nodes is smaller than $2\,\varepsilon$, then the jammer node is located at one of the two intersections of the circles around the target nodes with radius of ε each. Otherwise, the jammer node is always on the straight line that connects the two target nodes; that is, $\|\boldsymbol{z}^{\text{opt}} - \boldsymbol{x}_1\| + \|\boldsymbol{z}^{\text{opt}} - \boldsymbol{x}_2\| = \|\boldsymbol{x}_2 - \boldsymbol{x}_1\|$. In this case, depending on the CRLB values, the jammer node can be either at a distance of ε from one of the target nodes (the one with the lower CRLB) or at larger distances than ε from both of the target nodes. In the first scenario, the optimal jammer position is simply obtained as $\boldsymbol{z}^{\text{opt}} = \boldsymbol{x}_i + (\boldsymbol{x}_k - \boldsymbol{x}_i)\varepsilon/\|\boldsymbol{x}_k - \boldsymbol{x}_i\|$ when the jammer node is at a distance of ε from the ith target node. In the second scenario, an *equalizer* solution is observed as the CRLBs are equated, and the optimal jammer location is calculated as $\boldsymbol{z}^{\text{opt}} = \boldsymbol{x}_1 + (\boldsymbol{x}_2 - \boldsymbol{x}_1)d^*/\|\boldsymbol{x}_2 - \boldsymbol{x}_1\|$, where d^* is obtained from (4.9).

4.3 Special Case: Infinitesimally Small ε

In this section, the optimal location of the jammer node is investigated for $N_T \geq 3$ in the absence of constraints on the distances between the jammer node and the target nodes; that is, it is assumed that the constraints in (4.5) are ineffective. In this scenario, various theoretical results can be obtained related to the optimal location for the jammer node.

Remark 3: *The ineffectiveness of the distance constraints can naturally arise in some cases due to the max-min nature of the problem; that is, the solution of the problem in* (4.5) *can be the same in the presence and absence of the constraints (see Chapter 6 for examples). In addition, for applications in which small (e.g., 'nano size' [17]) jammer nodes with low powers are employed, the jammer node becomes difficult to detect; hence, it can be placed closely to the target nodes, leading to a low value of* ε *in* (4.5).

First, the following result is obtained to restrict the possible region for the optimal jammer location.

Proposition 4: *Suppose that* $N_T \geq 3$ *and* $\varepsilon \to 0$. *Then, the optimal location of the jammer node lies on the convex hull formed by the locations of the target nodes.*

Proof. Let $\mathcal{H}$ denote the convex hull formed by the locations of the target nodes; that is, $\mathcal{H} = \text{Conv}(\boldsymbol{x}_1, \ldots, \boldsymbol{x}_{N_T}) = \left\{ \sum_{i=1}^{N_T} \upsilon_i \, \boldsymbol{x}_i \,|\, \sum_{i=1}^{N_T} \upsilon_i = 1, \upsilon_i \geq 0, i = 1, \ldots, N_T \right\}$. By definition, $\mathcal{H}$ is a nonempty closed convex set. Let $\boldsymbol{z}_1$ be any point outside $\mathcal{H}$. Then, by the projection theorem [45], there exits a unique vector $\boldsymbol{z}_2$ in $\mathcal{H}$ that is closest to $\boldsymbol{z}_1$; that is, $\boldsymbol{z}_2 = \text{argmin}_{\boldsymbol{z} \in \mathcal{H}} \|\boldsymbol{z} - \boldsymbol{z}_1\|$ (i.e., $\boldsymbol{z}_2$ is the *projection* of $\boldsymbol{z}_1$ onto $\mathcal{H}$). The projection theorem also states that $\boldsymbol{z}_2$ is the projection of $\boldsymbol{z}_1$ onto $\mathcal{H}$ if and only if $(\boldsymbol{z}_1 - \boldsymbol{z}_2)^T (\boldsymbol{z}_3 - \boldsymbol{z}_2) \leq 0$ for all $\boldsymbol{z}_3 \in \mathcal{H}$ [45]. This condition can also be stated as

$$\boldsymbol{z}_1^T \boldsymbol{z}_3 - \boldsymbol{z}_1^T \boldsymbol{z}_2 - \boldsymbol{z}_2^T \boldsymbol{z}_3 + \|\boldsymbol{z}_2\|^2 \leq 0 \,. \tag{4.10}$$

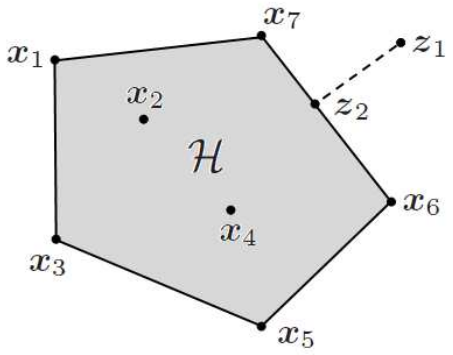

Figure 4.1: A scenario with $N_T = 7$ target nodes, where $\mathcal{H}$ denotes the convex hull formed by the locations of the target nodes (the gray area). Point $\boldsymbol{z}_2$ is the projection of $\boldsymbol{z}_1$ onto $\mathcal{H}$.

Multiplying the terms in (4.10) by 2 and moving some of the terms to the other side, the following inequality is obtained:

$$2\boldsymbol{z}_1^T\boldsymbol{z}_2 - \|\boldsymbol{z}_2\|^2 \geq 2\boldsymbol{z}_1^T\boldsymbol{z}_3 + \|\boldsymbol{z}_2\|^2 - 2\boldsymbol{z}_2^T\boldsymbol{z}_3 \ . \tag{4.11}$$

Since $\boldsymbol{z}_1 \notin \mathcal{H}$ and $\boldsymbol{z}_2 \in \mathcal{H}$, $\|\boldsymbol{z}_1 - \boldsymbol{z}_2\| > 0$ is satisfied, which is equivalent to $\|\boldsymbol{z}_1\|^2 > 2\boldsymbol{z}_1^T\boldsymbol{z}_2 - \|\boldsymbol{z}_2\|^2$. Then, from (4.11), the following relation is derived:

$$\|\boldsymbol{z}_1\|^2 > 2\boldsymbol{z}_1^T\boldsymbol{z}_3 + \|\boldsymbol{z}_2\|^2 - 2\boldsymbol{z}_2^T\boldsymbol{z}_3 \ . \tag{4.12}$$

Adding $\|\boldsymbol{z}_3\|^2$ to both sides of the inequality in (4.12), and rearranging the terms, the following distance relation is achieved:

$$\|\boldsymbol{z}_1 - \boldsymbol{z}_3\| > \|\boldsymbol{z}_2 - \boldsymbol{z}_3\| \tag{4.13}$$

for all $\boldsymbol{z}_3 \in \mathcal{H}$. Hence, for any point $\boldsymbol{z}_1$ outside $\mathcal{H}$, its projection onto $\mathcal{H}$, denoted by $\boldsymbol{z}_2$, is closer to any point $\boldsymbol{z}_3$ on $\mathcal{H}$. Therefore, the optimal jammer location cannot be outside the convex hull $\mathcal{H}$ formed by the locations of the target nodes as the CRLB for each target node is inversely proportional to the distance between the jammer and the target nodes. □

The statement in Proposition 4 is illustrated in Fig. 4.1. As stated in the proof of the proposition, for each location $\boldsymbol{z}_1$ outside the convex hull $\mathcal{H}$ (formed by the locations of the target nodes), its projection $\boldsymbol{z}_2$ onto $\mathcal{H}$ is closer to all the

locations on $\mathcal{H}$, hence, to all the target nodes. Therefore, the optimal jammer location must be always on the convex hull generated by the target nodes.

In [46], a semidefinite programming (SDP) relaxation based method is proposed for localization of target nodes in the absence of jamming, and it is observed that target nodes should be in the convex hull of the anchor nodes in order to perform accurate localization. However, this observation is different from the result in Proposition 4 in terms of both the considered problem and the employed proof technique.

Towards the aim of characterizing the optimal jammer location for $N_T > 3$, the scenario with $N_T = 3$ is investigated first. Consider a network with target nodes ℓ_1, ℓ_2, and ℓ_3 (i.e., $N_T = 3$). The max-min CRLB in the absence of distance constraints is defined as

$$\mathrm{CRLB}_{\ell_1,\ell_2,\ell_3} \triangleq \max_{\boldsymbol{z}} \min_{m\in\{\ell_1,\ell_2,\ell_3\}} \mathrm{CRLB}_m(\boldsymbol{z}) \tag{4.14}$$

where $\mathrm{CRLB}_m(\boldsymbol{z})$ is given by (cf. (4.5))

$$\mathrm{CRLB}_m(\boldsymbol{z}) \triangleq R_m \left(\frac{K_m P_J}{\|\boldsymbol{z} - \boldsymbol{x}_m\|^\nu} + \frac{N_0}{2} \right) . \tag{4.15}$$

According to Proposition 4, the optimal jammer location lies on the triangle formed by the locations of target nodes ℓ_1, ℓ_2, and ℓ_3. In particular, the jammer node can be either inside the triangle or on the boundary of the triangle.[2] For the former case, the following proposition presents the equalizer nature of the optimal solution.

Proposition 5: *Consider a network with three target nodes (i.e., $N_T = 3$). If the optimal jammer location obtained from* (4.14) *belongs to the interior of the convex hull (triangle) formed by the locations of the target nodes, then the CRLBs for the target nodes are equalized by the optimal solution.*

Proof. See Appendix A.3. □

[2]If the target nodes are co-linear, then the jammer node resides on the boundary of the 'triangle', which in fact reduces to a straight line segment.

Based on Proposition 5, it is concluded that if the optimal jammer location obtained from (4.14) belongs to the interior of the convex hull (triangle) formed by the three target nodes, then the resulting CRLBs for the target nodes are all equal. To investigate the scenario in which the optimal jammer location is on the boundary of the triangle formed by target nodes ℓ_1, ℓ_2, and ℓ_3, $\mathrm{CRLB}_{m,n}$ is defined as

$$\mathrm{CRLB}_{m,n} \triangleq \max_{\boldsymbol{z}} \min\{\mathrm{CRLB}_m(\boldsymbol{z}), \mathrm{CRLB}_n(\boldsymbol{z})\} \tag{4.16}$$

where $\mathrm{CRLB}_m(\boldsymbol{z})$ and $\mathrm{CRLB}_n(\boldsymbol{z})$ are given by (4.15). First, based on Proposition 3, the following result is obtained for two target nodes ($N_T = 2$) in the absence of distance constraints (i.e., $\varepsilon \to 0$).

Corollary 1: *For two target nodes and without distance constraints on the location of the jammer node, the optimal jammer location (see* (4.16)*) is on the straight line segment that connects the target nodes, and the CRLBs for the target nodes are equalized by the optimal solution.*

Proof. Consider Proposition 3 with $\varepsilon \to 0$. Then, the only possible scenario is (ii)–(c), which results in an equalizer solution with the jammer node being located on the straight line segment that connects the target nodes. □

Then, the following proposition characterizes the scenario in which the optimal jammer location according to (4.14) is on the boundary of the triangle formed by the target nodes.

Proposition 6: *Consider a network with target nodes ℓ_1, ℓ_2, and ℓ_3, and suppose that* $\mathrm{CRLB}_{\ell_1,\ell_2}$ *is the minimum of* $\{\mathrm{CRLB}_{\ell_1,\ell_2}, \mathrm{CRLB}_{\ell_1,\ell_3}, \mathrm{CRLB}_{\ell_2,\ell_3}\}$ *(see* (4.16)*).*[3] *Also, let $\boldsymbol{z}^{\mathrm{opt}}_{\ell_1,\ell_2}$ represent the optimizer of* (4.16) *for $m = \ell_1$ and $n = \ell_2$. Then, the optimal jammer location obtained from* (4.14) *satisfies the following properties:*

a) *If the optimal jammer location is on the boundary of the triangle formed by target nodes ℓ_1, ℓ_2, and ℓ_3, then the optimizer of* (4.14) *is equal to $\boldsymbol{z}^{\mathrm{opt}}_{\ell_1,\ell_2}$, and the*

[3] *It is possible to extend the results to scenarios in which* $\mathrm{CRLB}_{\ell_1,\ell_2}$ *is not a unique minimum.*

CRLBs for target nodes ℓ_1 and ℓ_2 are equalized by the optimal solution; that is, $\mathrm{CRLB}_{\ell_1}(\boldsymbol{z}^{\mathrm{opt}}_{\ell_1,\ell_2}) = \mathrm{CRLB}_{\ell_2}(\boldsymbol{z}^{\mathrm{opt}}_{\ell_1,\ell_2})$.

b) *The optimal location for the jammer node is on the boundary of the convex hull (triangle) formed by target nodes ℓ_1, ℓ_2, and ℓ_3 if and only if*

$$\|\boldsymbol{x}_{\ell_3} - \boldsymbol{z}^{\mathrm{opt}}_{\ell_1,\ell_2}\| \leq \sqrt[\nu]{P_J K_{\ell_3} \left(\frac{\mathrm{CRLB}_{\ell_1,\ell_2}}{R_{\ell_3}} - \frac{N_0}{2} \right)^{-1}}. \tag{4.17}$$

Proof. See Appendix A.5. □

Proposition 6 presents a necessary and sufficient condition for the optimal jammer location to be on the boundary of the convex hull (triangle) formed by the three target nodes (see (4.17)) in the absence of distance constraints. To utilize the results in Proposition 6, $\mathrm{CRLB}_{\ell_1,\ell_2}$, $\mathrm{CRLB}_{\ell_1,\ell_3}$, and $\mathrm{CRLB}_{\ell_2,\ell_3}$ are calculated from (4.16), and the condition in (4.17) is checked. If the condition holds, the optimal location for the jammer node is obtained as specified in Part a) of the proposition, which results in equalization of the CRLBs for (at least) two of the target nodes. Otherwise, the optimal location for the jammer node belongs to the interior of the convex hull, and the result in Proposition 5 applies.

Based on Propositions 4–6, the following result is obtained to characterize the optimal location for the jammer node for $N_T > 3$ and in the absence of distance constraints.

Proposition 7: *Suppose that $N_T > 3$ and $\varepsilon \to 0$. Let the max-min CRLB in the presence of target nodes ℓ_1, ℓ_2, and ℓ_3 only be denoted by* $\mathrm{CRLB}_{\ell_1,\ell_2,\ell_3}$, *which is as expressed in* (4.14). *Assume that target nodes i, j, and k achieve the minimum of* $\mathrm{CRLB}_{\ell_1,\ell_2,\ell_3}$ *for $\ell_1, \ell_2, \ell_3 \in \{1, \ldots, N_T\}$ and $\ell_1 \neq \ell_2 \neq \ell_3$, and let $\boldsymbol{z}^{\mathrm{opt}}_{i,j,k}$ denote the optimizer of* (4.14) *corresponding to* $\mathrm{CRLB}_{i,j,k}$; *that is, for $(\ell_1, \ell_2, \ell_3) = (i, j, k)$. Then, the optimal location for the jammer node (i.e., the optimizer of* (4.5) *in the absence of the distance constraints) is equal to $\boldsymbol{z}^{\mathrm{opt}}_{i,j,k}$, and at least two of the CRLBs of the target nodes are equalized by the optimal solution.*

Proof. See Appendix A.6. □

The significance of Proposition 7 is related to the statement that the optimal location of the jammer node is determined by no more than three of the target nodes for infinitesimally small ε. In addition, when the optimal location of the jammer node is obtained based on Proposition 7 as $\boldsymbol{z}_{i,j,k}^{\text{opt}}$, it also becomes the solution of (4.5) if $\boldsymbol{z}_{i,j,k}^{\text{opt}}$ is an element of $\{\boldsymbol{z} \,|\, \|\boldsymbol{z} - \boldsymbol{x}_i\| \geq \varepsilon\,,\ i = 1, \ldots, N_T\}$. Otherwise, (4.5) results in a different solution.

Finally, the following corollary is obtained based on Propositions 5–7.

Corollary 2: *Consider the scenario in Proposition 7 and suppose that the optimal location for the jammer node, $\boldsymbol{z}_{i,j,k}^{\text{opt}}$, belongs to the interior of the convex hull formed by target nodes i, j, and k. In addition, let $\text{CRLB}_{i,j}$ be the minimum of $\text{CRLB}_{i,j}$, $\text{CRLB}_{i,k}$, and $\text{CRLB}_{j,k}$, which are as defined in (4.16), and let $\boldsymbol{z}_{i,j}^{\text{opt}}$ represent the jammer location corresponding to $\text{CRLB}_{i,j}$. Then, $\boldsymbol{z}_{i,j,k}^{\text{opt}}$ cannot be inside any of the circles centered at target nodes i, j, and k with radii $\|\boldsymbol{x}_i - \boldsymbol{z}_{i,j}^{\text{opt}}\|$, $\|\boldsymbol{x}_j - \boldsymbol{z}_{i,j}^{\text{opt}}\|$, and d_{thr}, respectively, where*

$$d_{\text{thr}} \triangleq \sqrt[\nu]{P_J K_k \left(\frac{\text{CRLB}_{i,j}}{R_k} - \frac{N_0}{2}\right)^{-1}}\,. \tag{4.18}$$

Proof. See Appendix A.7. □

The statement in Corollary 2 is illustrated in Fig. 4.2. According to Corollary 2, the jammer node cannot be inside any of the three circles shown in the figure, and the only feasible region is the shaded area. This corollary is useful to reduce the search region for the optimal location of the jammer node.

Based on the theoretical results in this section, the following algorithm can be proposed for calculating the optimal location of the jammer node, $\boldsymbol{z}^{\text{opt}}$, for the generic problem in (4.5):

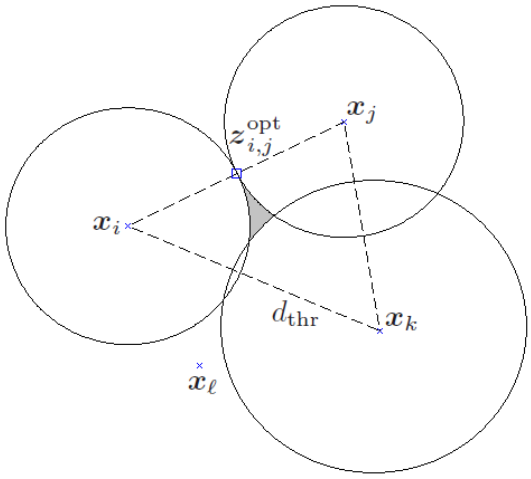

Figure 4.2: The scenario in Corollary 2, where the optimal location for the jammer node corresponds to a point in the shaded (gray) area.

Algorithm 1

- If $N_T = 1$, $\boldsymbol{z}^{\text{opt}}$ can be chosen to be any point at a distance of ε from the target node.
- If $N_T = 2$, $\boldsymbol{z}^{\text{opt}}$ can be obtained from Proposition 3, which presents either a closed-form solution, or a solution based on a simple one-dimensional search (see (4.9)).
- If $N_T \geq 3$,
  - If the conditions in Proposition 1 hold, $\boldsymbol{z}^{\text{opt}}$ is at a distance of ε from a specific target node.
  - If the conditions in Proposition 2 hold, $\boldsymbol{z}^{\text{opt}}$ is determined by two of the target nodes, as described in Proposition 3.
  - Otherwise,
    - For each distinct group of three target nodes, say ℓ_1, ℓ_2, and ℓ_3,
      - Calculate the pairwise CRLBs in (4.16) considering the equalizer property in Corollary 1, and determine the minimum of them, say $\text{CRLB}_{\ell_1,\ell_2}$.

- If the condition in (4.17) of Proposition 6 holds, set $\mathrm{CRLB}_{\ell_1,\ell_2,\ell_3}$ to $\mathrm{CRLB}_{\ell_1,\ell_2}$.
- Otherwise, obtain $\mathrm{CRLB}_{\ell_1,\ell_2,\ell_3}$ from (4.14) under the equalizer constraint specified in Proposition 5.

* Determine the minimum of the $\mathrm{CRLB}_{\ell_1,\ell_2,\ell_3}$ terms and the corresponding optimal location, $\boldsymbol{z}_{\mathrm{unc}}^{\mathrm{opt}}$ (i.e., the optimal location in the absence of distance constraints).
* If $\boldsymbol{z}_{\mathrm{unc}}^{\mathrm{opt}}$ is feasible according to (4.5), then $\boldsymbol{z}^{\mathrm{opt}} = \boldsymbol{z}_{\mathrm{unc}}^{\mathrm{opt}}$. Otherwise, solve (4.5) directly to obtain $\boldsymbol{z}^{\mathrm{opt}}$.

It should be noted that the solution of (4.5) requires a two-dimensional search over the set of feasible locations for the jammer node. On the other hand, the algorithm based on Propositions 5–7 involves $\binom{N_T}{3}$ optimization problems, each of which is over a one-dimensional space due to the equalizer properties in the propositions. In the worst case where (4.5) is solved exhaustively, $N_F N_T$ evaluations of the CRLB expression in (4.3) is required, with N_F denoting the number of feasible locations in the environment (considering a certain resolution for the search). On the other hand, in the best case, Proposition 1 can be applied and the optimal jammer location can be obtained with no more than $(N_T)^2$ CRLB evaluations (see (4.6)).

Chapter 5

Extensions

In practical localization systems, an anchor node can be connected to a target node if the signal-to-noise ratio (SNR) at the receiver of the target node is larger than a certain threshold. Since the jammer node degrades the SNRs at the target nodes, it may be possible in some cases that the set of anchor nodes that are connected to a target node can change with respect to the location of the jammer node. In order to incorporate such cases, the problem formulation in the previous sections can be generalized as follows: Let $\mathcal{A}_i$ in Chapter 2 now represent the set of anchor nodes that are connected to the ith target node *in the absence of jamming*. In addition, let SNR_{ij} denote the SNR of the received signal coming to target node i from anchor node j, which can be expressed as $\mathrm{SNR}_{ij} = E_{ij}/(K_i P_J/\|\boldsymbol{z} - \boldsymbol{x}_i\|^\nu + N_0/2)$, where E_{ij} is the energy of the signal coming from anchor node j (i.e., the energy of the first term in (2.1)) and $K_i P_J/\|\boldsymbol{z} - \boldsymbol{x}_i\|^\nu + N_0/2$ is the sum of the spectral density levels of the jammer noise (cf. (4.2)) and the measurement noise. Then, the condition that SNR_{ij} is above a threshold, $\mathrm{SNR}_{\mathrm{thr}}$, can be expressed, after some manipulation, as follows:

$$\|\boldsymbol{z} - \boldsymbol{x}_i\| > \left(\frac{K_i P_J}{E_{ij}/\mathrm{SNR}_{\mathrm{thr}} - N_0/2}\right)^{1/\nu} \triangleq d_{ij}^{\mathrm{lim}} \tag{5.1}$$

for $i \in \{1, \ldots, N_T\}$ and $j \in \mathcal{A}_i$, where $E_{ij}/\mathrm{SNR}_{\mathrm{thr}} > N_0/2$ holds for $j \in \mathcal{A}_i$ by definition. The inequality in (5.1) states that if the distance between the jammer node and target node i is larger than a critical distance d_{ij}^{lim}, then target node i

can utilize the signal coming from anchor node j; otherwise, target node i cannot communicate with anchor node j. In this scenario, the CRLB expressions can be updated by incorporating these conditions into (3.5) as follows:

$$\boldsymbol{J}_i(\boldsymbol{x}_i, P_J) = \sum_{j \in \mathcal{A}_i^L} \frac{\lambda_{ij} \mathbb{I}_{\{\|\boldsymbol{z}-\boldsymbol{x}_i\| > d_{ij}^{\lim}\}}}{N_0/2 + P_J |\gamma_{ij}|^2} \boldsymbol{\phi}_{ij} \boldsymbol{\phi}_{ij}^T \tag{5.2}$$

where $\mathbb{I}$ denotes an indicator function, which is equal to one when the condition is satisfied and zero otherwise. From (5.2), the CRLB in (4.3) and (4.4) can be expressed, via (4.2), as

$$\mathrm{CRLB}_i(d_i) = R_i(d_i) \left(K_i P_J/(d_i)^\nu + N_0/2\right) \tag{5.3}$$

where $d_i \triangleq \|\boldsymbol{z} - \boldsymbol{x}_i\|$ and

$$R_i(d_i) \triangleq \mathrm{tr} \left\{ \left[\sum_{j \in \mathcal{A}_i^L} \lambda_{ij} \mathbb{I}_{\{d_i > d_{ij}^{\lim}\}} \boldsymbol{\phi}_{ij} \boldsymbol{\phi}_{ij}^T \right]^{-1} \right\}. \tag{5.4}$$

Based on the new CRLB expression in (5.3) and (5.4), the extensions of the theoretical results in Chapter 4 can be investigated as follows: Proposition 1 can directly be applied by replacing the condition in (4.6) with the following:

$$\mathrm{CRLB}_\ell(\varepsilon) \leq \min_{\substack{i \in \{1,\ldots,N_T\} \\ i \neq \ell}} \mathrm{CRLB}_i(\|\boldsymbol{x}_i - \boldsymbol{x}_\ell\| + \varepsilon). \tag{5.5}$$

Similarly, Proposition 2 can be employed by using the following inequality instead of (4.8): $\mathrm{CRLB}_m(\|\boldsymbol{z}_{k,i}^{\mathrm{opt}} - \boldsymbol{x}_m\|) \geq \mathrm{CRLB}_{k,i}$, where $\mathrm{CRLB}_{k,i}$ denotes the solution of (4.7) when R_i in the objective function is as defined in (5.4). Regarding Proposition 3, Part (i) directly applies, and Part (ii)–(a) and Part (ii)–(b) are valid when the definition of R_i is updated. However, Part (ii)–(c) does not directly apply since equalization may not be possible due to the discontinuous nature of the CRLB expression in (5.3) and (5.4). Hence, in this scenario, instead of (4.9), the following conditions should be employed for d^*:

$$\begin{aligned} \mathrm{CRLB}_1(d) &\geq \mathrm{CRLB}_2(\|\boldsymbol{x}_1 - \boldsymbol{x}_2\| - d) \ \text{ for } d < d^* \\ \mathrm{CRLB}_1(d) &\leq \mathrm{CRLB}_2(\|\boldsymbol{x}_1 - \boldsymbol{x}_2\| - d) \ \text{ for } d > d^* \end{aligned} \tag{5.6}$$

Proposition 4 can also be directly applied under the assumption that the jammer node cannot disable all the target nodes from a location outside the convex hull

(that is, the minimum CRLB of the target nodes should be finite for all jammer locations outside the convex hull). Regarding Propositions 5–7, the continuity property of the CRLB plays an important role for proving the results in these propositions. Therefore, they do not apply in general for the CRLB expression in (5.3) and (5.4). To extend the results in Propositions 5–7, a continuous approximation of the CRLB expression can be considered. From (5.4), it is noted that the CRLB can have finitely many discontinuities, the number of which is determined by the number of anchor nodes. Hence, by approximating the CRLB from below (so that it is still a lower bound) around those discontinuities leads to an approximate formulation for which the results in Propositions 5–7 can be applied. Investigation of such approximations and their practical implications are considered as a direction for future work.

Remark 4: The theoretical results in this thesis are valid not only for the CRLB expressions that are derived based on the considered system model but also for any localization accuracy metric that satisfies the following properties: (*i*) The localization accuracy improves as the distance between the jammer node and the target node increases. (*ii*) The localization accuracy metric is a continuous function of the distance between the jammer node and the target node. In particular, Propositions 1, 2, 3, 4 and Corollary 1 can directly be extended when condition (*i*) is satisfied. On the other hand, the results in Propositions 5, 6, 7 and Corollary 2 are valid when both condition (*i*) and (*ii*) are satisfied. Since the first property should hold for any reasonable average performance metric for localization, the results in Propositions 1, 2, 3, 4 and Corollary 1 can be considered to be valid for generic system and jamming models.

Chapter 6

Numerical Examples

In this chapter, the theoretical results in Chapter 4 are illustrated via numerical examples. The parameters in (4.5) are set to $\varepsilon = 1\,\mathrm{m.}$, $N_0 = 2$, $\nu = 2$, and $K_i = 1$ for $i = 1, \ldots, N_T$, and the jammer power P_J is normalized as $\bar{P}_J = 2P_J/N_0$. For each target node, LOS connections to all the anchor nodes are assumed, and R_i in (4.5) is calculated via (4.4) based on (3.7) and the following expression: $\lambda_{ij} = 100\|\boldsymbol{x}_i - \boldsymbol{y}_j\|^{-2}$; that is, the free space propagation model is considered as in [40].

First, a network consisting of four anchor nodes ($N_A = 4$) and three target nodes ($N_T = 3$) is investigated, where the node locations are as illustrated in Fig. 6.1. For this scenario, when $\bar{P}_J = 6$, Proposition 2 can be applied as follows: $\mathrm{CRLB}_{\ell_1,\ell_2}$'s are calculated from (4.7), and $\mathrm{CRLB}_{k,i}$ with $k = 1$ and $i = 3$ is found to be the minimum one. Then, it is shown that the conditions in Proposition 2 are satisfied for $k = 1$ and $i = 3$, which means that the solution of the whole network (i.e., the solution of (4.5)) is determined by the subnetwork consisting of target node 1 and target node 3. Then, Proposition 3 is invoked, and the optimal location of the jammer node and the corresponding max-min CRLB are calculated as $\boldsymbol{z}_{1,3}^{\mathrm{opt}} = [4.8713\ 4.5898]\,\mathrm{m.}$ and $\mathrm{CRLB}_{1,3} = 0.9279\,\mathrm{m}^2$, respectively, based on Proposition 3-*(ii)-(c)*. In Fig. 6.1, the optimal locations of the jammer node are also shown (via the green line) for various values of $\bar{P}_J$ ranging from 0.5

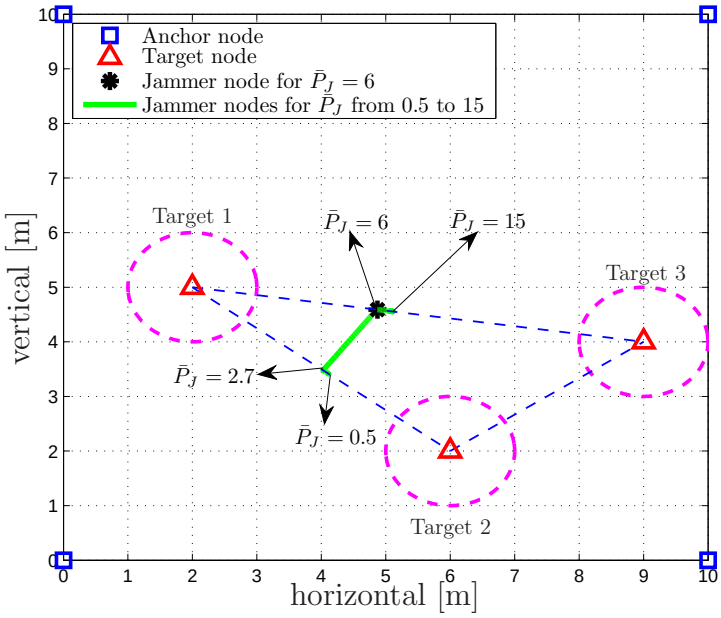

Figure 6.1: The network consisting of anchor nodes at [0 0], [10 0], [0 10], and [10 10] m., and target nodes at [2 5], [6 2], and [9 4] m.

to 15. In this scenario, the condition in Proposition 6-(b) is satisfied for $\ell_1 = 1$ and $\ell_2 = 2$ when $\bar{P}_J$ is lower than 2.7, and for $\ell_1 = 1$ and $\ell_2 = 3$ when $\bar{P}_J$ is higher than 5.8, which imply that the optimal jammer location is determined by target nodes 1 and 2 for $\bar{P}_J < 2.7$, and by target nodes 1 and 3 for $\bar{P}_J > 5.8$, as described in Proposition 6-(a). For the remaining values of $\bar{P}_J$, the condition in Proposition 6-(b) is not satisfied, which implies that the solution belongs to the interior of the triangle formed by the locations of all the target nodes and that the CRLBs for all the target nodes are equalized as a result of Proposition 5. It should be noted that since the distances between the target nodes and the optimal locations of the jammer node are larger than $\varepsilon = 1$ m. (that is, the constraints in (4.5) are ineffective), the solution of (4.5) is equivalent to that obtained in the absence of the distance constraints; hence, the results in Propositions 4-7 can be invoked. In Fig. 6.2, individual CRLBs of all the target nodes and the max-min CRLB of the whole network are plotted versus the normalized jammer power. From the figure, it is observed that the max-min CRLB of the whole network is equal to the CRLBs of target nodes 1 and 2 for $\bar{P}_J < 2.7$, and is equal to the

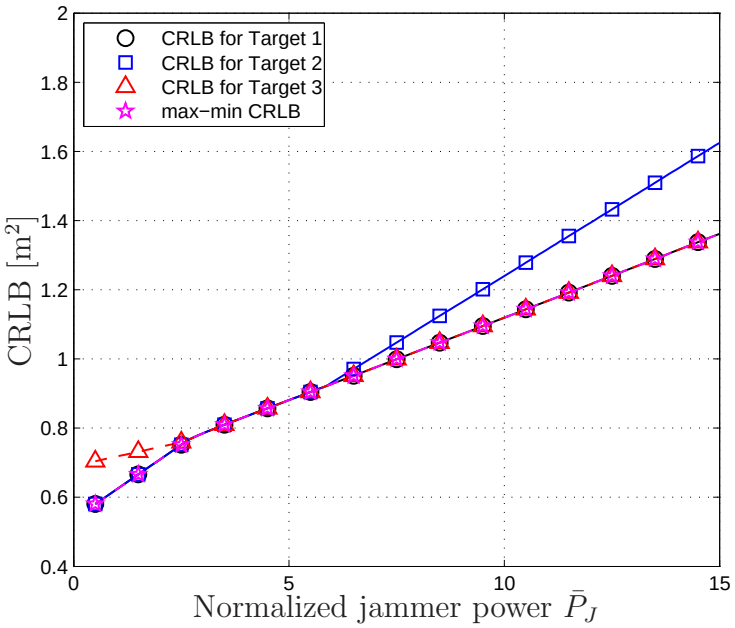

Figure 6.2: CRLB corresponding to each target node and max-min CRLB for the whole network for the scenario in Fig. 6.1.

CRLBs of target nodes 1 and 3 for $\bar{P}_J > 5.8$ in accordance with Proposition 6. For the other values of $\bar{P}_J$, the CRLBs of all the target nodes are equalized in accordance with Proposition 5 and Proposition 6.

Next, another scenario with four anchor nodes and four target nodes is investigated, where the node locations are as shown in Fig. 6.3. For $\bar{P}_J = 6$, when Proposition 7 is employed in this scenario, it is observed that the subnetwork consisting of target nodes 1, 3, and 4 achieves the minimum max-min CRLB among all possible subnetworks with three target nodes. In addition, the condition in Proposition 6-(b) is not satisfied, which implies that $\boldsymbol{z}_{1,3,4}^{\text{opt}}$ belongs to the interior of the convex hull (triangle) formed by the locations of target nodes 1, 3, and 4; hence, as stated by Proposition 5, the CRLBs of target nodes 1, 3, and 4 are equalized. Accordingly, the corresponding values are obtained as $\text{CRLB}_{1,3,4} = 0.7983\,\text{m}^2$ and $\boldsymbol{z}_{1,3,4}^{\text{opt}} = [5.5115\ 5.5717]\,\text{m}.$, and the calculations show that the CRLB for target node 2 is larger than $\text{CRLB}_{1,3,4}$ for the optimal jammer location. Also, according to Corollary 2, the optimal location of the jammer

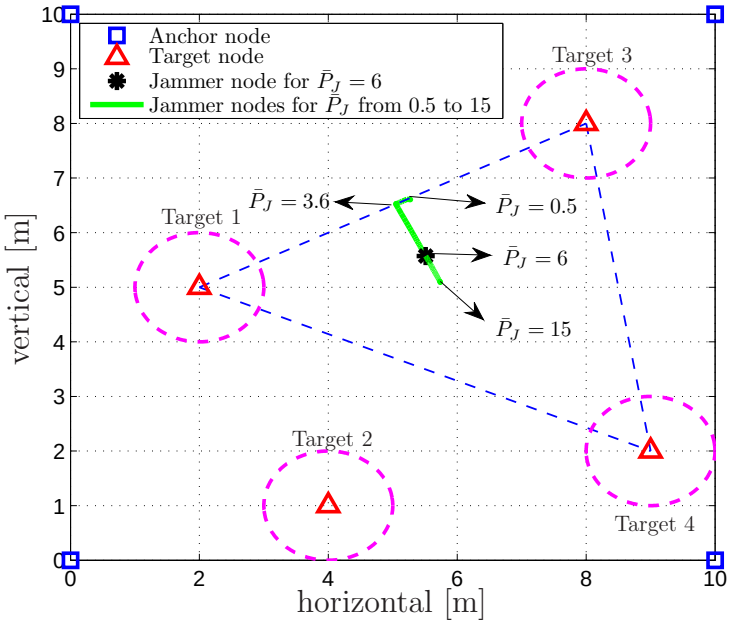

Figure 6.3: The network consisting of anchor nodes at [0 0], [10 0], [0 10], and [10 10] m., and target nodes at [2 5], [4 1], [8 8], and [9 2] m.

node cannot be inside any of the circles centered at target nodes 1, 3, and 4 with radii $\|\boldsymbol{x}_1 - \boldsymbol{z}_{1,3}^{\text{opt}}\|$, $\|\boldsymbol{x}_3 - \boldsymbol{z}_{1,3}^{\text{opt}}\|$, and d_{thr}, respectively, which is confirmed by Fig. 6.4. Hence, Corollary 2 can be useful for reducing the search space for the optimal location of the jammer node. Since the distances between the target nodes and $\boldsymbol{z}_{1,3,4}^{\text{opt}}$ are larger than $\varepsilon = 1$ m.; that is, $\boldsymbol{z}_{1,3,4}^{\text{opt}}$ is an element of $\{\boldsymbol{z} \,|\, \|\boldsymbol{z} - \boldsymbol{x}_i\| \geq \varepsilon\,,\ i = 1, 2, 3, 4\}$, the solution of (4.5) is the same as that of the subnetwork consisting of target nodes 1, 3, and 4 in this scenario. In Fig. 6.3, the optimal location of the jammer node is also investigated for the values of $\bar{P}_J$ ranging from 0.5 to 15 (the green line in the figure). Proposition 7 indicates that the subnetwork consisting of target nodes 1, 3, and 4 achieves the minimum max-min CRLB among all possible subnetworks with three target nodes for all values of $\bar{P}_J$ in this range. It is also observed that the condition in part (b) of Proposition 6 is satisfied with $\ell_1 = 1$ and $\ell_2 = 3$ for the values of $\bar{P}_J$ lower than 3.6, which implies that the solution is determined by target nodes 1 and 3 for $\bar{P}_J < 3.6$ as specified by part (a) of Proposition 6. For the other values of $\bar{P}_J$, the condition in Proposition 6-(b) is not satisfied, indicating that the solution

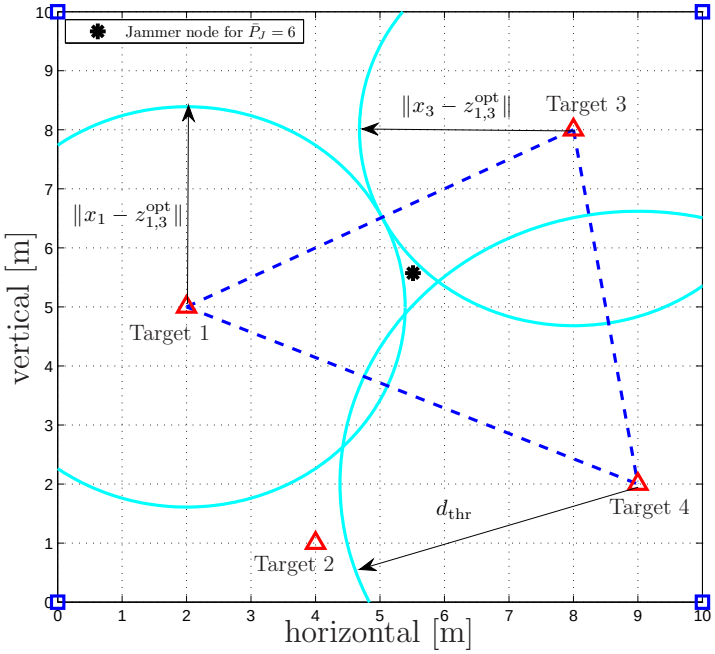

Figure 6.4: Illustration of Corollary 2 for the scenario in Fig. 6.3.

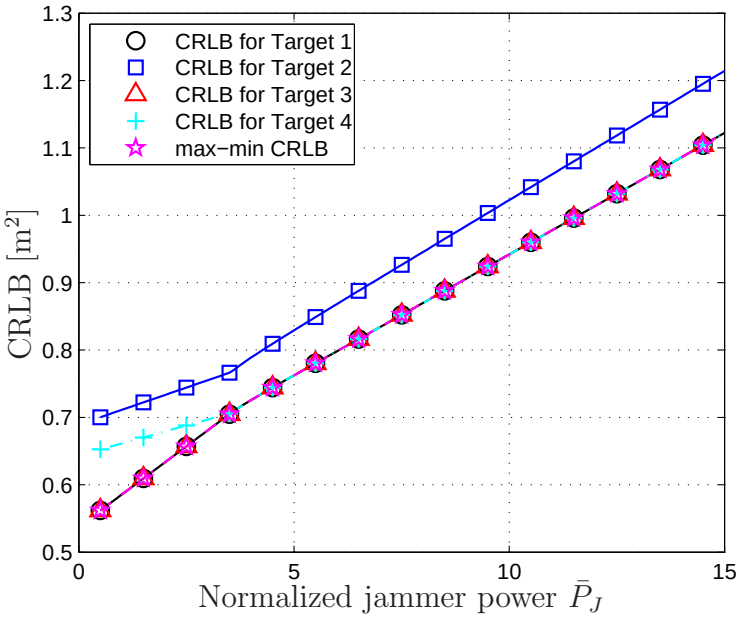

Figure 6.5: CRLB corresponding to each target node and max-min CRLB for the whole network for the scenario in Fig. 6.3.

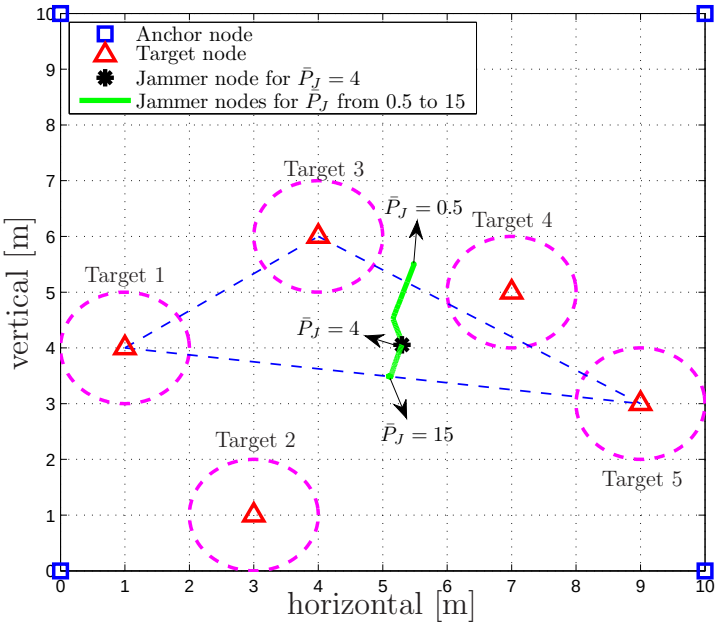

Figure 6.6: The network consisting of anchor nodes at [0 0], [10 0], [0 10], and [10 10] m., and target nodes at [1 4], [3 1], [4 6], [7 5], and [9 3] m.

belongs to the interior of the triangle formed by the locations of target nodes 1, 3, and 4, and the CRLBs of target nodes 1, 3, and 4 are equalized in accordance with Proposition 5. In Fig. 6.5, the CRLBs of the target nodes and the max-min CRLB of the whole network are plotted versus the normalized jammer power for the values of $\bar{P}_J$ ranging from 0.5 to 15. In accordance with the previous findings, based on Proposition 5, Proposition 6, and Proposition 7, the CRLBs of target nodes 1 and 3 are equalized to the max-min CRLB of the whole network when $\bar{P}_J$ is lower than 3.6, and for the other values of $\bar{P}_J$ the CRLBs of target nodes 1, 3, and 4 are equalized to the max-min CRLB of the whole network.

In the final scenario, the network in Fig. 6.6 with four anchor nodes and five target nodes is considered. Via Proposition 7, it is calculated for $\bar{P}_J = 4$ that the subnetwork consisting of target nodes 1, 3, and 5 achieves the minimum max-min CRLB among all possible subnetworks with three target nodes, and by checking the condition in Proposition 6-(b), it is shown that $\boldsymbol{z}_{1,3,5}^{\text{opt}}$ belongs to the interior of the convex hull (triangle) formed by the locations of target nodes 1, 3, and 5, and

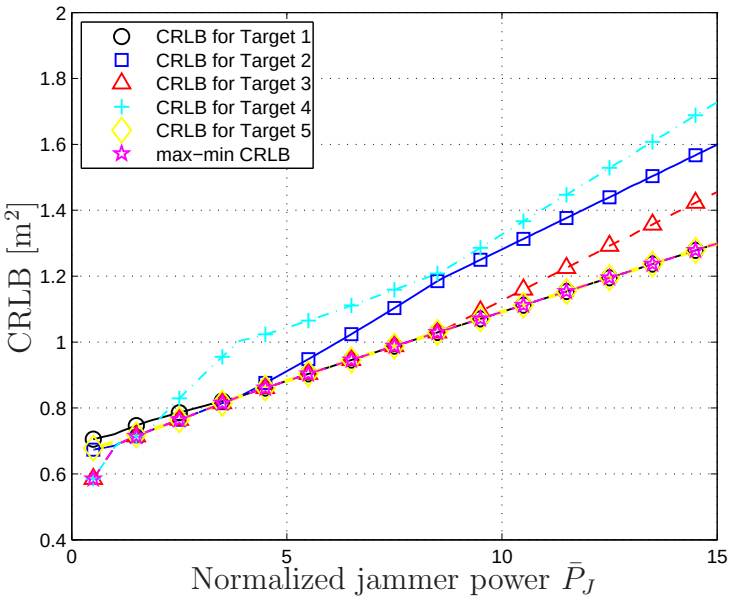

Figure 6.7: CRLB corresponding to each target node and max-min CRLB for the whole network for the scenario in Fig. 6.6.

the CRLBs of target nodes 1, 3, and 5 are equalized in compliance with Proposition 5 (see the algorithm at the end of Section IV.). In accordance with these findings, the corresponding values are obtained as $\mathrm{CRLB}_{1,3,5} = 0.8392\,\mathrm{m}^2$ and $\boldsymbol{z}_{1,3,5}^{\mathrm{opt}} = [5.2987\ 4.0537]\,\mathrm{m}.$, and the CRLBs for the other target nodes are shown to be larger than $\mathrm{CRLB}_{1,3,5}$ for the optimal jammer location. In this scenario, similar to the previous scenarios, $\boldsymbol{z}_{1,3,5}^{\mathrm{opt}}$ is an element of $\{\boldsymbol{z} \,|\, \|\boldsymbol{z}-\boldsymbol{x}_i\| \geq \varepsilon\,,\ i = 1,2,3,4,5\}$; hence, the solution of (4.5) is the same as that of the subnetwork consisting of target nodes 1, 3, and 5. Corollary 2 imposes that the optimal location of the jammer node cannot be inside any of the circles centered at target nodes 1, 3, and 5 with radii $\|\boldsymbol{x}_1 - \boldsymbol{z}_{1,5}^{\mathrm{opt}}\|$, d_{thr}, and $\|\boldsymbol{x}_5 - \boldsymbol{z}_{1,5}^{\mathrm{opt}}\|$, respectively, which can easily be verified in this example. In Fig. 6.6, the optimal location of the jammer node is also shown for the values of $\bar{P}_J$ ranging from 0.5 to 15. In compliance with Proposition 7, the subnetwork consisting of target nodes 2, 3, and 4 achieves the minimum max-min CRLB among all possible subnetworks with three target nodes for the values of $\bar{P}_J$ lower than 1.7, the subnetwork consisting of target nodes 2, 3, and 5 achieves the minimum max-min CRLB for $\bar{P}_J$ between 1.7 and

3.9, and the subnetwork consisting of target nodes 1, 3, and 5 achieves the minimum max-min CRLB for $\bar{P}_J$ above 3.9. Since the distances between the target nodes and the optimal location of the jammer node are larger than $\varepsilon = 1\,\mathrm{m}$. for all $\bar{P}_J$ in this scenario, the solution of (4.5) is the same as those of the aforementioned subnetworks for the respective ranges of $\bar{P}_J$. Considering the values of $\bar{P}_J$ lower than 1.7, the condition in Proposition 6-(b) is satisfied with $\ell_1 = 3$ and $\ell_2 = 4$ for $\bar{P}_J < 1.1$, which implies that the solution is determined by target nodes 3 and 4 for $\bar{P}_J < 1.1$ as described in Proposition 6-(a), and for $1.1 \leq \bar{P}_J < 1.7$ by Proposition 6-(b) the optimal jammer location is shown to belong to the interior of the triangle formed by the locations of target nodes 2, 3, and 4, and the CRLBs of target nodes 2, 3, and 4 are equalized due to Proposition 5. Similarly, based on Propositions 5 and 6, it can be shown for $1.7 \leq \bar{P}_J \leq 3.9$ that the optimal jammer location belongs to the interior of the triangle formed by the locations of the target nodes 2, 3, and 5, and that the CRLBs of target nodes 2, 3, and 5 are equalized. In a similar fashion, it can be shown for $\bar{P}_J > 3.9$ that the optimal location of the jammer node is determined only by target nodes 1 and 5 for $\bar{P}_J \geq 8.5$ as described in Proposition 6-(a), and for $3.9 < \bar{P}_J < 8.5$ it belongs to the interior of the triangle formed by the locations of target nodes 1, 3, and 5, which results in the equalization of the CRLBs of target nodes 1, 3, and 5. In Fig. 6.7, the CRLBs of all the target nodes and the max-min CRLB of the whole network are plotted versus the normalized jammer power for the values of $\bar{P}_J$ ranging from 0.5 to 15. All the previous findings are confirmed by this figure.

To analyze the effects of the SNR on the jamming performance, the max-min CRLBs for the networks in Fig. 6.1, Fig. 6.3, and Fig. 6.6 are plotted in Fig. 6.8 versus the spectral density level of the measurement noise, N_0, where $P_J = 10$ is employed. As expected, an increase in N_0 (equivalently, a decrease in the SNR) results in a higher max-min CRLB. Since the network geometries in Fig. 6.1, Fig. 6.3, and Fig. 6.6 are similar to one another (that is, in particular, the anchor nodes are located at the same positions), the max-min CRLBs for all the three networks are close to each other, as observed from Fig. 6.8. However, there also exist some variations due to the differences in the numbers and configurations of the target nodes.

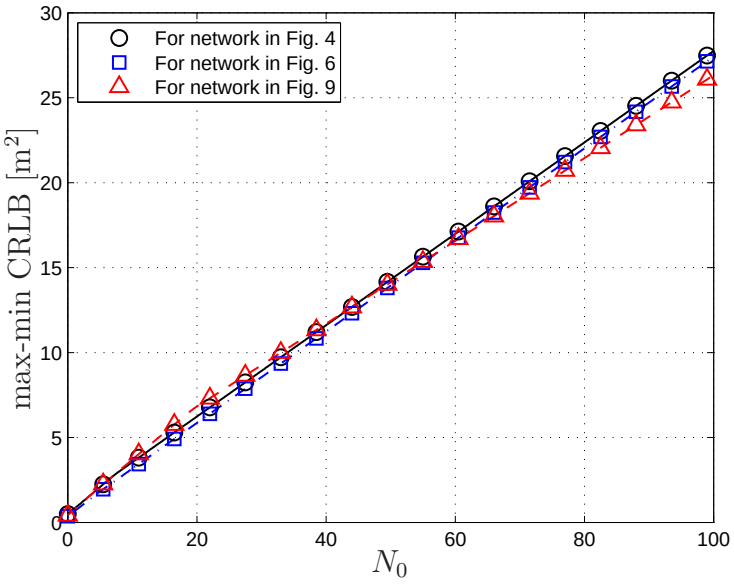

Figure 6.8: Max-min CRLB for the networks in Fig. 6.1, Fig. 6.3, and Fig. 6.6 versus the spectral density level of the measurement noise, N_0, where $P_J = 10$.

For the network in Fig. 6.1, the minimum CRLB of the target nodes is plotted versus the location of the jammer node in Fig. 6.9, where $N_0 = 2$ and $\bar{P}_J = 10$ in Fig. 6.9-(a) and $N_0 = 50$ and $\bar{P}_J = 10$ in Fig. 6.9-(b). In the first scenario, the optimal location of the jammer node is given by $\boldsymbol{z}_{\text{opt}} = (5.031, 4.567)\,\text{m}.$ where the CRLBs of the target nodes 1 and 3 are equalized as specified by Proposition 6. On the other hand, in the second scenario, the optimal jammer location is $\boldsymbol{z}_{\text{opt}} = (4.14, 3.394)\,\text{m}.$ and the CRLBs of the target nodes 1 and 2 are equalized in accordance with Proposition 6. From Fig. 6.9 and the location constraints shown in Fig. 6.1, the nonconvexity of the optimization problem in (4.5) can be observed clearly. In addition, it is noted that the minimum CRLB becomes more sensitive to the location of the jammer node when the spectral density level of the measurement noise is lower; that is, the minimum CRLB changes by larger factors with respect to the jammer location in Fig. 6.9-(a).

In order to investigate the optimal jammer placement problem based on the CRLB expression in (5.3) and (5.4) in Chapter 5, consider a critical SNR level for the receivers of the target nodes as $\text{SNR}_{\text{thr}} = 1$ (i.e., $0\,\text{dB}$). In addition, let the

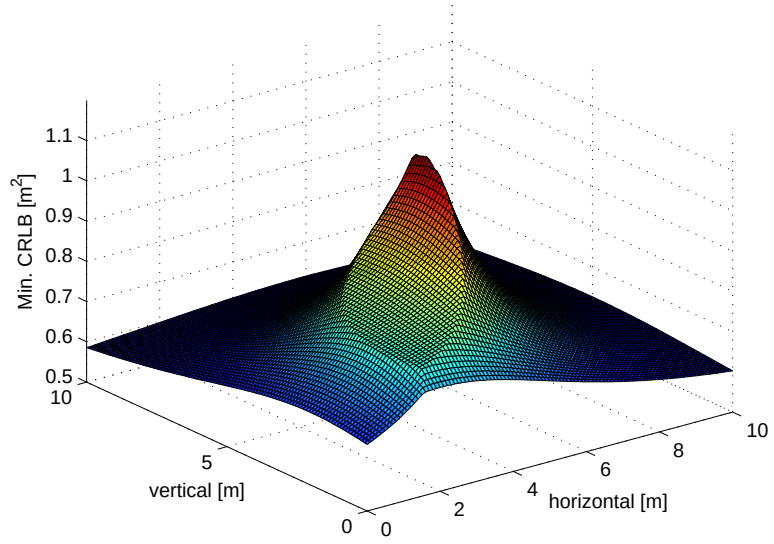

(a)

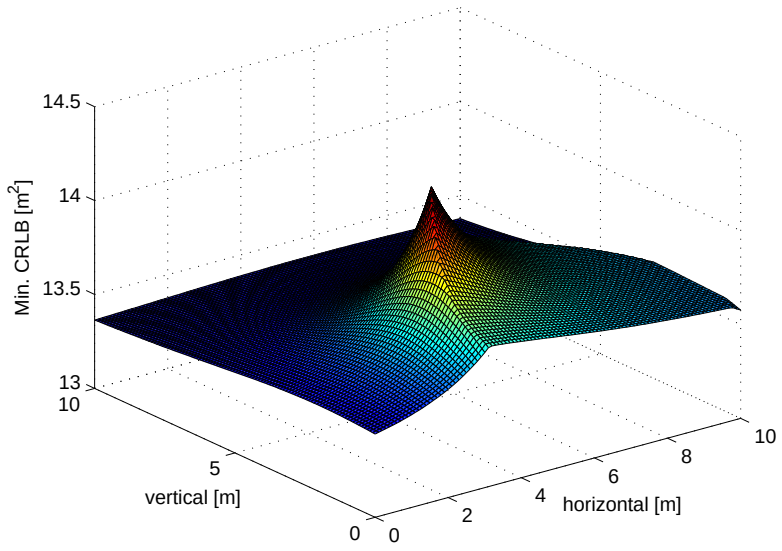

(b)

Figure 6.9: The minimum CRLB of the target nodes versus the location of the jammer node for (a) $N_0 = 2$ and (b) $N_0 = 50$, where $P_J = 10$.

E_{ij} parameter in (5.1) be given by $E_{ij} = 2000/\|\boldsymbol{x}_i - \boldsymbol{y}_j\|^2$. Then, it can be shown that the critical distances, $d_{ij}^{\lim}$, are lower than $\varepsilon = 1\,\mathrm{m}$. (cf. (4.1)) in all the cases considered in the previous numerical examples. Hence, the results are valid for the CRLB expression in (5.3) and (5.4), as well. To provide an example in which the differences due to the CRLB expression in Chapter 5 can be observed, reconsider the network in Fig. 6.1 in the presence of higher powers for the jammer node. Fig. 6.10 illustrates the CRLBs for the target nodes, together with the max-min CRLB, where the optimal locations for the jammer node are obtained based on the CRLB expression in (5.3) and (5.4). For comparison purposes, the max-min CRLB corresponding to the optimal locations for the jammer node obtained from the CRLB expression in (4.3) and (4.4) is also illustrated in the figure (labeled as "original"). It is noted that there exist discontinuities in the CRLBs due to the fact that the connections between the anchor and target nodes are lost when the SNRs get below the critical SNR level (cf. (5.3) and (5.4)). Also, up to $\bar{P}_J = 338.5$, the max-min CRLBs with and without the consideration of lost connections take the same values. Considering that both of the max-min CRLBs achieve the value of $17.23\,\mathrm{m}^2$ just before $\bar{P}_J = 338.5$ and that the maximum distance between the anchor nodes is equal to $10\sqrt{2}\,\mathrm{m}$ in the network, it can be concluded that the extended formulation based on the CRLB expression in (5.3) and (5.4) reduces to the original formulation based on the CRLB expression in (4.3) and (4.4) for the practical ranges of localization accuracy in this example (i.e., the differences are observed only for the cases in which the localization accuracy is unacceptable for practical applications). From Fig. 6.10, it is also observed that the CRLBs of target node 2, 1, and 3 go to infinity at $\bar{P}_J = 419.5$, $\bar{P}_J = 468.6$, and $\bar{P}_J = 747.1$, respectively, due to the loss of connections to the anchor nodes. As a result, the max-min CRLB becomes infinity after $\bar{P}_J = 747.1$. Table 6.1 presents the optimal jammer locations according to both formulations for various values of the normalized jammer power. It is noted that the change in the optimal location of the jammer node with respect to $\bar{P}_J$ is relatively noticeable according to the extended formulation compared to that according to the original formulation, for which the change is almost indiscernible.

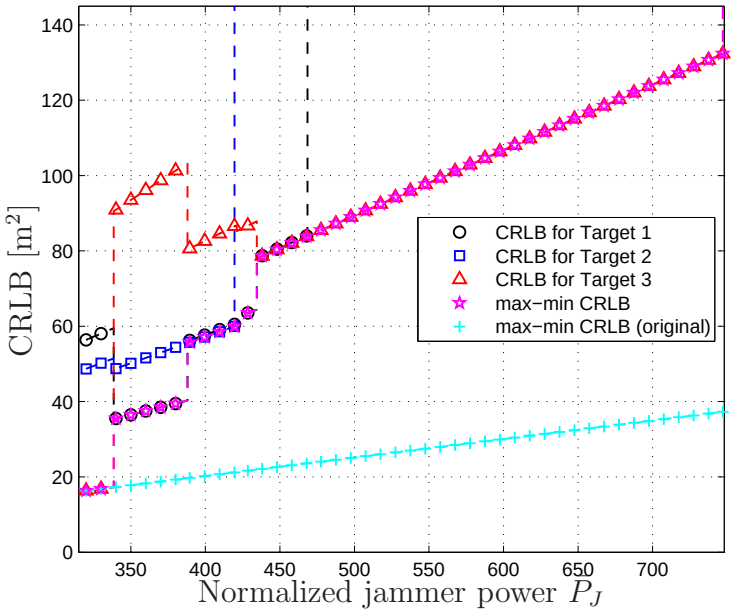

Figure 6.10: CRLB of each target node and the max-min CRLB of the network for the scenario in Fig. 6.1, where the optimal locations for the jammer node are obtained based on the CRLB expression in (5.3) and (5.4). The max-min CRLB corresponding to the optimal locations based on the CRLB expression in (4.3) and (4.4) is also shown ('original').

Table 6.1: The optimal location of the jammer node according to the original and extended formulations for the scenario in Fig. 6.1.

P_J	Original formulation	Extended formulation
320	(5.2802, 4.5314) m.	(5.2802, 4.5314) m.
339	(5.2807, 4.5313) m.	(5.4610, 4.5046) m.
420	(5.2822, 4.5311) m.	(4.9232, 4.7215) m.
470	(5.2829, 4.5310) m.	(4.6000, 4.6286) m.
747	(5.2849, 4.5306) m.	(4.6092, 4.6286) m.

Chapter 7

A Numerical Algorithm

In this chapter, a numerical and recursive algorithm is proposed to determine the optimal jammer location in wireless localization systems. The problem is to determine the jammer position at which the minimum CRLB among the CRLBs of all the target nodes takes its maximum value. Each point in the two-dimensional space is a candidate for the optimal position in general. To solve the problem numerically and in a computationally efficient manner, an algorithm is proposed.

The problem formulation in (4.5) leads to a non-convex problem. Therefore, it is not possible to use the convex optimization tools to determine the optimal jammer location. To solve the problem, an exhaustive search over all the feasible points is required, in general. For instance, if the grid-based algorithm is used, the continuous sensor field is divided into smaller grids and after placing the jammer node at each feasible grid point, the CRLBs of all the target nodes are calculated and the minimum CRLB is determined. The grid point with the highest minimum CRLB is declared as the optimal jammer location. However, to determine the optimal jammer location more accurately, the grid size needs to be reduced in general. As the grid size is reduced, the computational effort to solve the problem increases significantly. For practical systems, in which the position of the jammer node needs to be changed dynamically, this may bring a huge computational burden to the system. Thus, a more efficient algorithm is proposed to solve the

optimization problem.

7.1 Description of the Algorithm

In the algorithm, a proper initial position is chosen to place the jammer node. Then, the position of the jammer is updated during the iterations. The jammer is always moved in accordance with the objective function of the problem. Since the objective is to maximize the minimum CRLB based on the location of the jammer, the jammer node is moved with the purpose of increasing the CRLB(s) of the target node(s) with the minimum CRLB at each iteration. The jammer movements are simple: it is moved on a straight line at each iteration. The points at which the jammer node is located during the iterations of the algorithm compose the jammer path. Since the candidate positions for the optimal jammer location are restricted with the jammer path, the search space is greatly reduced with the proposed algorithm in most of the cases.

Due to the location constraints in (4.5) for the jammer node, each target node has an ε-radius circular area around it and these regions are not allowed for locating the jammer node (except the boundaries). Since the points composing the jammer path are candidates for the optimal location, they also satisfy the location constraints. Furthermore, it is assumed that the distance between each pair of target nodes is at least 2ε, i.e., there is no intersection between the ε-radius circles around the target nodes.

If the jammer node is placed at one of the nearest possible points to a target node and after this placement, that target node has the minimum CRLB in the system, then the jammer is located optimally, as stated in Proposition 1. To be able to exploit this fact, the jammer is initially located at the intersection of the ε-radius circle around the target node that has the minimum CRLB before jammer placement ($T_{min}^{(0)}$) and the straight line segment between $T_{min}^{(0)}$ and the target node with the second minimum CRLB ($T_{min2}^{(0)}$). The following equation

gives the initial position of the jammer node:

$$\mathbf{z}^{(1)} = \mathbf{x}_{min}^{(0)} + (\mathbf{x}_{min2}^{(0)} - \mathbf{x}_{min}^{(0)})\varepsilon / \|\mathbf{x}_{min2}^{(0)} - \mathbf{x}_{min}^{(0)}\| \tag{7.1}$$

After initial placement of the jammer, if the same target node has the minimum CRLB, the algorithm ends; otherwise, iterations begin. Before the first iteration, the jammer is located on the ε-radius circle around $T_{min}^{(0)}$ and on the straight line segment between $T_{min}^{(0)}$ and the (new) target node with the minimum CRLB ($T_{min}^{(1)}$). $CRLB_i^{(k)}$ denotes the CRLB of target node i at the kth iteration and $CRLB_{min}^{(k)}$ represents the minimum CRLB in the system at the kth iteration. The jammer node is then moved one step size (δ) towards the target node with the minimum CRLB ($T_{min}^{(k)}$) along the straight line segment between the positions $\mathbf{z}^{(k)}$ and $\mathbf{x}_{min}^{(k)}$ of the jammer node and the target node with the minimum CRLB, respectively, as stated in Eq. (7.2). Then at each iteration, based on the new position of the jammer, the CRLB values of the target nodes are updated and the (new) target node with the minimum CRLB is determined.

$$\mathbf{z}^{(k+1)} = \mathbf{z}^{(k)} + (\mathbf{x}_{min}^{(k)} - \mathbf{z}^{(k)})\delta / \|\mathbf{x}_{min}^{(k)} - \mathbf{z}^{(k)}\| \tag{7.2}$$

If there exist more than one target nodes with the minimum CRLB in an iteration, the jammer should be moved in a way to increase the CRLBs of all the target nodes with the minimum CRLB. However, this may not always be possible. The set $S^{(k)}$ contains the target nodes which have the minimum CRLB at the kth iteration, which is expressed as

$$S^{(k)} = \{i \mid i \in \{1, \ldots, N_T\},\ CRLB_i^{(k)} = CRLB_{min}^{(k)}\}. \tag{7.3}$$

Let $Conv(S^{(k)})$ denote the convex hull formed by the locations of the target nodes with the minimum CRLB at the kth iteration of the algorithm, that is,

$$Conv(S^{(k)}) = \Big\{ \sum_{i \in S^{(k)}} \upsilon_i \, \mathbf{x}_i \,\Big|\, \sum_{i \in S^{(k)}} \upsilon_i = 1,\ \upsilon_i \geq 0, \forall i \in S^{(k)} \Big\} \tag{7.4}$$

If, at any iteration, the jammer node is in $Conv(S^{(k)})$, it is certain that after jammer movement in any direction, the CRLB of at least one of the target nodes with the minimum CRLB decreases (see the proof in Appendix A.8). In this

case, the jammer is moved towards one of the target nodes with the minimum CRLB. If the jammer is outside $Conv(S^{(k)})$, then it is moved towards the convex hull in the direction of the closest straight line segment between the jammer node and the convex hull, i.e., the jammer moves along the line segment between its position and its projection ($\mathbf{z}_{prj}^{(k)}$) onto $Conv(S^{(k)})$. By exploiting the projection theorem [45], it can be shown that the distances between the jammer node and all the target nodes with the minimum CRLB decrease so that the CRLBs of all the target nodes with the minimum CRLB increase as a result of this jammer movement.

According to the jammer movements described up to this point, the jammer path may intersect with ε-radius circles around the target nodes in some localization networks. In order to prevent the violation of the location constraints, different jammer movements must also be proposed. In the algorithm, firstly the target node that leads to the violation is determined. If the violation occurs at the kth iteration, this target node is denoted as $T_{vio}^{(k)}$ and its position is denoted as $\mathbf{x}_{vio}^{(k)}$. Then, the jammer node is moved one step size along the line perpendicular to the line segment between the jammer node and $T_{vio}^{(k)}$. Hence, nearly a tangential movement to the ε-radius circle around the violating target node is considered. Since the jammer can move in two opposite directions along this line, the direction that leads the jammer to be closer to $T_{min}^{(k)}$ (or $Conv(S^{(k)})$) is chosen. If there is again a violation of the location constraints in the new jammer position, in accordance with the actual route, the jammer is moved onto the ε-radius circle around $T_{vio}^{(k)}$ such that it lies on the line segment between $T_{vio}^{(k)}$ and $T_{min}^{(k)}$ (or the projection of $T_{vio}^{(k)}$ onto $Conv(S^{(k)})$, which is denoted as $\mathbf{x}_{vio,prj}^{(k)}$).

$CRLB_{min}$ represents the highest minimum CRLB value obtained until the kth iteration of the algorithm, and $\mathbf{z}^{alg}$ denotes the best jammer location found in the algorithm until the kth iteration, i.e., $\mathbf{z}^{alg}$ is the jammer location for which $CRLB_{min}$ is achieved. $CRLB_{min}$ and $\mathbf{z}^{alg}$ are stored in order to display them at the end. The iterations are terminated if the $CRLB_{min}$ value does not change for a certain number of iterations. More explicitly, if the $CRLB_{min}$ value stays constant during two consecutive iterations, a parameter (I_{nc}) is increased by one; otherwise it is set to zero. If the value of I_{nc} increases up to the value of a

predetermined parameter (I_{fnsh}), the algorithm is terminated, which indicates that more jammer movements are unlikely to increase $CRLB_{min}$.

The following proposition states that the proposed algorithm determines the optimal jammer location for an infinitesimally small step size and an infinitesimally small ε.

Proposition 8: *Assume that the minimum distance between any two target nodes in the system is nonzero (i.e., $\varrho > 0$). If for a given wireless localization network, the minimum CRLB of the target nodes as a function of the jammer location is unimodal, i.e., $f(z) = \min_{i\in\{1,\ldots,N_T\}} R_i\left(\frac{K_i P_J}{\|\boldsymbol{z}-\boldsymbol{x}_i\|^{\nu}} + \frac{N_0}{2}\right)$ has a single maximum, the algorithm converges almost surely to the optimal jammer location in the absence of location constraints and for an infinitesimally small step size; i.e., if $\varepsilon \to 0$ and $\delta \to 0$, then $\boldsymbol{z}^{alg} \to \boldsymbol{z}^{opt}$ as $k \to \infty$ where $\boldsymbol{z}^{opt}$ is the solution of the optimization problem in* (4.5).

Proof. See Appendix A.8. □

The significance of Proposition 8 is that the convergence to the max-min CRLB is obtained by the algorithm under some conditions for very low step sizes in the absence of location constraints for the jammer node. Since the max-min CRLB corresponds to the optimal jammer location, the algorithm solves the optimization problem numerically with its simple structure. In practice, since the step size cannot be chosen infinitesimally small due to the computational complexity considerations, it is possible to observe slight decrements in the level of the minimum CRLB in the system during some iterations of the algorithm. However, this generally does not lead the jammer node not to pass through the optimal jammer location along its path. It is numerically observed that the minimum CRLB value during the iterations of the algorithm has a general trend of increasing up to the iterations at which the jammer node gets close to the optimal location. After then, the minimum CRLB curve shows a fluctuating behavior about the highest minimum CRLB level since the jammer node moves around the optimal jammer location in the remaining iterations. The details of the algorithm are presented

in Algorithm 2 below.

Algorithm 2

Calculate $CRLB_i^{(0)}, \ \forall\, i \in \{1, \ldots, N_T\}$
Determine $T_{min}^{(0)}$ and $T_{min2}^{(0)}$
$\mathbf{z}^{(1)} = \mathbf{x}_{min}^{(0)} + (\mathbf{x}_{min2}^{(0)} - \mathbf{x}_{min}^{(0)})\varepsilon / \|\mathbf{x}_{min2}^{(0)} - \mathbf{x}_{min}^{(0)}\|$
Calculate $CRLB_i^{(1)}, \ \forall\, i \in \{1, \ldots, N_T\}$
Determine $T_{min}^{(1)}$ and $CRLB_{min}^{(1)}$
Set initial values as $CRLB_{min} = CRLB_{min}^{(1)}$ and $\mathbf{z}^{alg} = \mathbf{z}^{(1)}$
if $T_{min}^{(1)} \neq T_{min}^{(0)}$,
    $\mathbf{z}^{(2)} = \mathbf{x}_{min}^{(0)} + (\mathbf{x}_{min}^{(1)} - \mathbf{x}_{min}^{(0)})\varepsilon / \|\mathbf{x}_{min}^{(1)} - \mathbf{x}_{min}^{(0)}\|$
    Set $k = 2$ and $I_{nc} = 0$
    while $I_{nc} < I_{fnsh}$,
        Calculate $CRLB_i^{(k)}, \ \forall\, i \in \{1, \ldots, N_T\}$
        Determine $T_{min}^{(k)}$ and $CRLB_{min}^{(k)}$
        if $CRLB_{min}^{(k)} > CRLB_{min}$,
            $CRLB_{min} = CRLB_{min}^{(k)}$ and $\mathbf{z}^{alg} = \mathbf{z}^{(k)}$
            $I_{nc} = 0$
        else
            $I_{nc} = I_{nc} + 1$
        end if
        if $|S^{(k)}| \geq 2$ and $\mathbf{z}^{(k)} \notin Conv(S^{(k)})$,
            $\mathbf{z}^{(k+1)} = \mathbf{z}^{(k)} + (\mathbf{z}_{prj}^{(k)} - \mathbf{z}^{(k)})\delta / \|\mathbf{z}_{prj}^{(k)} - \mathbf{z}^{(k)}\|$
        else
            $\mathbf{z}^{(k+1)} = \mathbf{z}^{(k)} + (\mathbf{x}_{min}^{(k)} - \mathbf{z}^{(k)})\delta / \|\mathbf{x}_{min}^{(k)} - \mathbf{z}^{(k)}\|$
        end if
        if $\exists\, i$ such that $\|\mathbf{z}^{(k+1)} - \mathbf{x}_i\| < \varepsilon, \ \ i \in \{1, \ldots, N_T\}$,
            Set $T_{vio}^{(k)} = i$ and $\mathbf{x}_{vio}^{(k)} = \mathbf{x}_i$
            Find the unit vector $\hat{\mathbf{u}}$, such that $\hat{\mathbf{u}} \ \perp \ (\mathbf{x}_{vio}^{(k)} - \mathbf{z}^{(k)})$
            if $|S^{(k)}| \geq 2$ and $\mathbf{z}^{(k)} \notin Conv(S^{(k)})$,
                if $\|\mathbf{z}_{prj}^{(k)} - (\mathbf{z}^{(k)} + \hat{\mathbf{u}}\,\delta)\| \leq \|\mathbf{z}_{prj}^{(k)} - (\mathbf{z}^{(k)} - \hat{\mathbf{u}}\,\delta)\|$,

$\mathbf{z}^{(k+1)} = \mathbf{z}^{(k)} + \hat{\mathbf{u}}\,\delta$

else

$\mathbf{z}^{(k+1)} = \mathbf{z}^{(k)} - \hat{\mathbf{u}}\,\delta$

end if

if $\exists\, i$ such that $\|\mathbf{z}^{(k+1)} - \mathbf{x}_i\| < \varepsilon, \quad i \in \{1, \ldots, N_T\}$,

$\mathbf{z}^{(k+1)} = \mathbf{x}_{vio}^{(k)} + (\mathbf{x}_{vio,prj}^{(k)} - \mathbf{x}_{vio}^{(k)})\varepsilon / \|\mathbf{x}_{vio,prj}^{(k)} - \mathbf{x}_{vio}^{(k)}\|$

end if

else

if $\|\mathbf{x}_{min}^{(k)} - (\mathbf{z}^{(k)} + \hat{\mathbf{u}}\,\delta)\| \leq \|\mathbf{x}_{min}^{(k)} - (\mathbf{z}^{(k)} - \hat{\mathbf{u}}\,\delta)\|$,

$\mathbf{z}^{(k+1)} = \mathbf{z}^{(k)} + \hat{\mathbf{u}}\,\delta$

else

$\mathbf{z}^{(k+1)} = \mathbf{z}^{(k)} - \hat{\mathbf{u}}\,\delta$

end if

if $\exists\, i$ such that $\|\mathbf{z}^{(k+1)} - \mathbf{x}_i\| < \varepsilon, \quad i \in \{1, \ldots, N_T\}$,

$\mathbf{z}^{(k+1)} = \mathbf{x}_{vio}^{(k)} + (\mathbf{x}_{min}^{(k)} - \mathbf{x}_{vio}^{(k)})\varepsilon / \|\mathbf{x}_{min}^{(k)} - \mathbf{x}_{vio}^{(k)}\|$

end if

end if

end if

$k = k + 1$

end loop

end if

7.2 Performance Evaluation

In this section, the algorithm is tested for some wireless localization networks. In the simulations, for all the networks, there exist four anchor nodes located at the corners of a square area, namely, at [0 0], [10 0], [0 10], and [10 10] m. The jammer power parameter P_J is chosen to be 6 and the noise spectral power level N_0 is set to 2. The step size of the jammer movement at each iteration of the algorithm is taken as 0.001 m. I_{fnsh} is chosen as 10 so that if the highest minimum CRLB value stays constant for 10 iterations, then the iterations are terminated.

The network shown in Fig. 7.1-(a) contains three target nodes located at [2 1], [3 8], and [9 8] m. The triangles in Fig. 7.1-(a) represent the anchor nodes. The minimum allowed distance between a target and the jammer node is taken as $\varepsilon = 0.6$ m. In Fig. 7.1-(a), the ε-radius red circles around the target nodes represent the forbidden regions to place the jammer node. Unimodality of the minimum CRLB of the target nodes as a function of the jammer location is observed in Fig. 7.2; hence, for the given network the proposed numerical algorithm is expected to work well. The jammer is initially placed on the circle around the target node located at [3 8] m. along the straight line segment between the target nodes at [3 8] and [2 1] m. After 7538 iterations, the highest minimum CRLB value is obtained when the jammer node is located at [4.8123 5.1877] m. and the CRLBs of all the three target nodes are calculated as $0.7952\,m^2$ at this point. In Fig. 7.1-(a), the blue curve represents the jammer path and the square on the jammer path represents the best jammer location determined by the algorithm. Then, the grid-based exhaustive search method is used where the grid size is taken as 0.001 m. The highest minimum CRLB is searched by placing the jammer node at all feasible grid points, which are outside of the ε-radius circles around the target nodes. Then, the optimal grid point is obtained as [4.8120 5.1880] m. at which the CRLBs of all the three target nodes are calculated as $0.7952\,m^2$. Therefore, for the scenario given in Fig. 7.1, the proposed algorithm determines the optimal jammer location accurately. The grid-based algorithm searches for the optimal jammer location over approximately 9.66×10^7 grid points. Since the jammer path of the algorithm contains only 7538 points for this specific example, a considerable amount of computations is eliminated with the proposed algorithm. Fig. 7.1-(b) shows the minimum CRLB values calculated based on the jammer path shown in Fig. 7.1-(a). It is observed that the minimum CRLB generally increases along the jammer path until the optimal point is reached.

In the second network shown in Fig. 7.3-(a), there exist thirteen target nodes located at [1 1], [1 9], [2 6], [3 4], [4 8], [5 2], [6 4], [6 6], [7 9], [8 1], [8 3], [9 6], and [9 8] m., and ε is taken as 0.4 m. In Fig. 7.4, it is observed that the minimum CRLB of the target nodes versus the jammer location is a unimodal function. After 3081 iterations, the highest minimum CRLB is calculated when

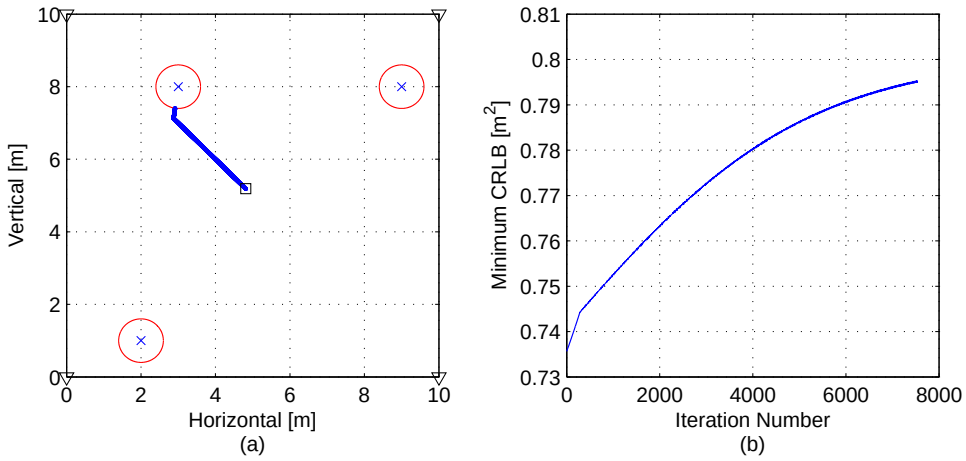

Figure 7.1: An illustration of the algorithm for a network in which the target nodes are at [2 1], [3 8], and [9 8] m. (a) The network and the jammer path. (b) The minimum CRLB in the system during the iterations of the algorithm.

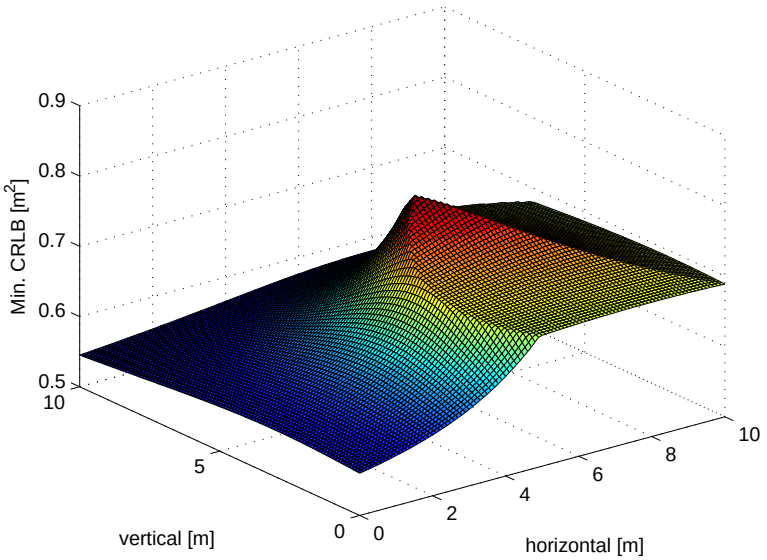

Figure 7.2: The minimum CRLB of the target nodes versus the location of the jammer node for the network given in Fig. 7.1-(a).

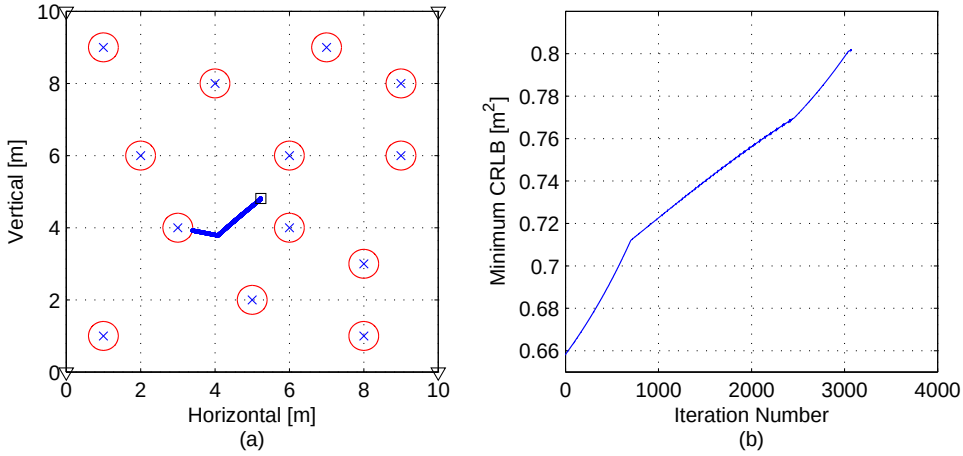

Figure 7.3: An illustration of the algorithm for a network in which the target nodes are at [1 1], [1 9], [2 6], [3 4], [4 8], [5 2], [6 4], [6 6], [7 9], [8 1], [8 3], [9 6], and [9 8] m. (a) The network and the jammer path. (b) The minimum CRLB in the system during the iterations of the algorithm.

the jammer node is located at [5.2313 4.8076] m. The CRLBs of the target nodes at this point are calculated as 0.8199, 0.8088, 0.8017, 0.9973, 0.8053, 0.9510, 2.8254, 1.9305, 0.8522, 0.8176, 0.8018, 0.9548, and $0.8017\,m^2$, respectively for the target node positions given above. Thus, the minimum CRLB is found as $0.8017\,m^2$. By having a grid-size of 0.001 m., the grid-based exhaustive search algorithm calculates the highest minimum CRLB as $0.8017\,m^2$ when the jammer node is placed at [5.2310 4.8080] m. Thus, for the network given in Fig. 7.3, the proposed algorithm works well. The exhaustive search algorithm seeks the optimal jammer location over approximately 9.35×10^7 grid points. The proposed algorithm searches for the optimal jammer location over 3081 points; hence, it is computationally far more efficient. In Fig. 7.3-(b) the minimum CRLB curve is shown for the jammer path illustrated in Fig. 7.3-(a).

The third network is presented in Fig. 7.5-(a), which contains five target nodes located at [1 7], [4 2], [5 4], [6 2], and [8 5] m. The minimum CRLB of the target nodes is plotted versus the location of the jammer node in Fig. 7.6. From this figure, unimodality of the minimum CRLB function is observed. The location constraint parameter is chosen as $\varepsilon = 0.8$ m., i.e., tighter security measurements

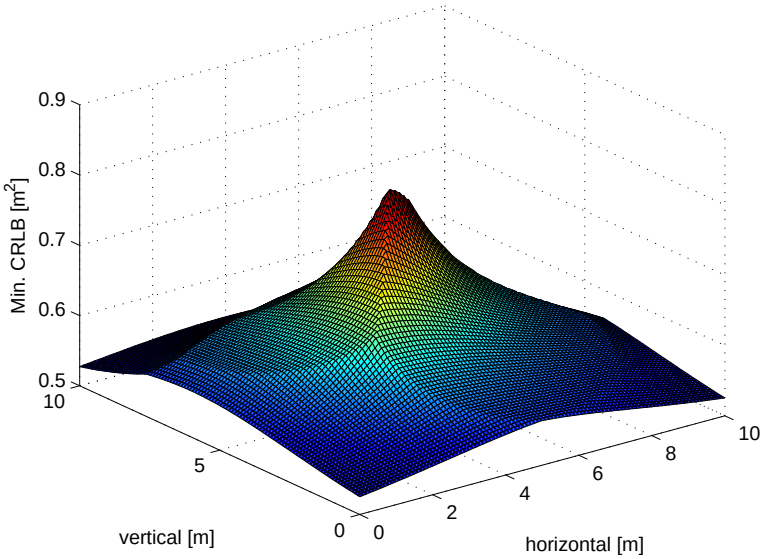

Figure 7.4: The minimum CRLB of the target nodes versus the location of the jammer node for the network presented in Fig. 7.3-(a).

are considered compared to the previous networks. The initial location of the jammer is on the ε-radius circle around the target node located at [5 4] m. and on the straight line segment between the target nodes located at [5 4] and [8 5] m. During some iterations, in order not to violate the location constraints, as proposed in the algorithm, the jammer node makes nearly tangential movements to the ε-radius circle around target node located at [5 4] m. After 1461 iterations, $\mathbf{z}^{alg}$ is determined as [4.8395 4.8673] m. The CRLBs of the target nodes at this point are calculated as 0.8663, 0.8903, 4.2870, 0.8663, and 0.8663 m^2, respectively. Thus, the minimum CRLB is found as 0.8663 m^2. With the grid-based algorithm and the grid size being equal to 0.001 m., the highest minimum CRLB value is obtained as 0.8662 m^2 where the jammer node is located at [4.8390 4.8670] m. It is then concluded that for the network given in Fig. 7.5, the proposed algorithm determines the optimal jammer location accurately. The grid-based exhaustive search algorithm looks for the optimal location over approximately 8.99×10^7 grid points. On the other hand, the jammer path includes 1461 points. Hence, for the given scenario, the computational complexity is considerably reduced with the proposed algorithm. Fig. 7.5-(b) shows the minimum CRLB levels accordingly

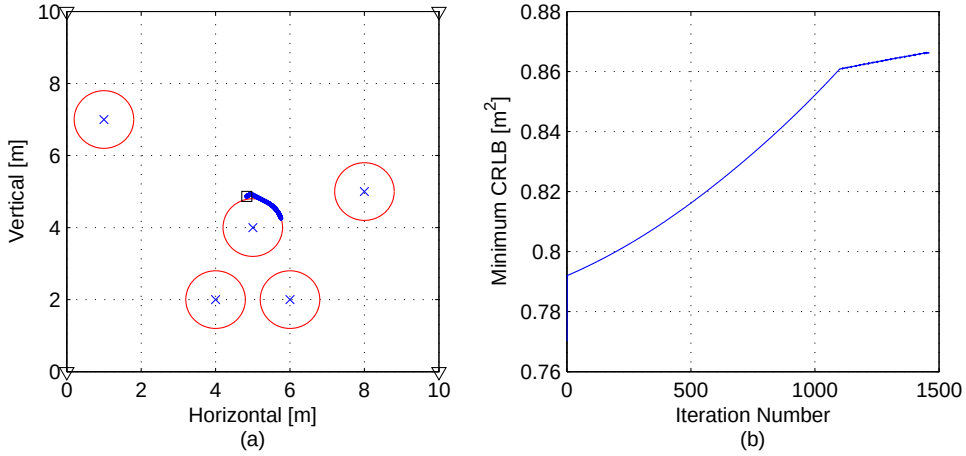

Figure 7.5: An illustration of the algorithm for a network in which the target nodes are at [1 7], [4 2], [5 4], [6 2], and [8 5] m. (a) The network and the jammer path. (b) The minimum CRLB in the system during the iterations of the algorithm.

to the jammer path shown in Fig. 7.5-(a).

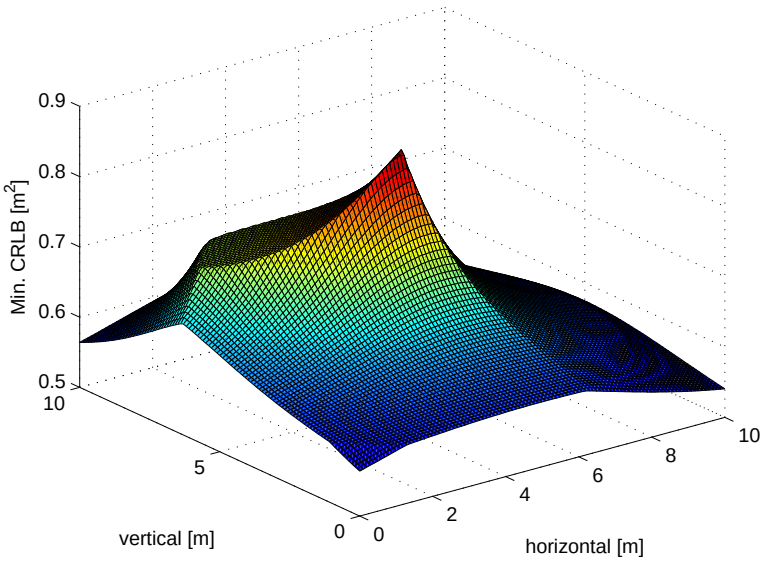

Figure 7.6: The minimum CRLB of the target nodes versus the location of the jammer node for the network presented in Fig. 7.5-(a).

Chapter 8

Concluding Remarks

The problem of optimal jammer placement has been proposed for maximizing the minimum of the CRLBs for a number of target nodes in a wireless localization system. Theoretical results have been obtained for specifying scenarios in which the jammer node is located as close to a certain target node as possible, or the optimal location of the jammer node is determined by two of the target nodes. Also, explicit expressions for the optimal location of the jammer node have been derived in the presence of two target nodes. In the absence of distance constraints for the jammer node, it has been shown that the optimal jammer location lies on the convex hull formed by the locations of the target nodes, equalizes the CRLBs of at least two of the target nodes, and is determined by two or three of the target nodes. Numerical examples have provided an illustration of the theoretical results in different scenarios. Performing experiments to evaluate the effects of jamming and to investigate the optimal location for a jammer node in a practical wireless localization system can be considered as an important direction for future work.

In addition to the theoretical results, a numerical algorithm has been proposed for optimally placing a jammer node in a wireless localization network. The algorithm has a simple structure, which is intuitive and easy to implement. The need for such an algorithm is due to the fact that the existing numerical methods for determining the optimal jammer location may require a brute-force technique.

Also, based on the presented theoretical results, a direct solution of the problem is required in the worst case. Then, the computational effort and the required time to find the optimal jammer location may be huge depending on the desired accuracy. Especially, for the localization systems used for tracking target nodes, the location of the jammer node may be updated dynamically. For such systems, simpler algorithms are required in general. With the proposed algorithm, it has been shown that the computational complexity is significantly reduced and the accuracy in determining the optimal location is very high. In fact, it has been proved that the algorithm converges to the optimal jammer location under certain conditions. The algorithm can be extended to the multi-jammer case in which the joint optimization of the locations and the power levels of jammer nodes is required. Furthermore, the computational complexity can be reduced further by changing the step size adaptively during the iterations of the algorithm.

Based on the results in this thesis, various guidelines can be provided related to jamming mitigation in wireless localization systems. Since the solution of the optimal jammer placement problem (cf. (4.5)) corresponds to the maximum degradation that can be caused by a jammer node, the transmitted powers of the anchor nodes in the wireless localization system can be adjusted accordingly in order to satisfy certain accuracy requirements in all scenarios. (A target node can measure the received noise level in certain intervals to determine the presence and power level of the jammer node.) In addition, for applications in which the anchor nodes can be moved, the locations of the anchor nodes (hence, the geometry of the system) can be adapted for reducing the effectiveness of jamming (cf. (4.4)). Furthermore, if possible, additional anchor nodes can be employed depending on the required localization accuracy and the severity of jamming.

Although the jammer node is assumed to know all the localization related parameters in this study, the results can also be extended to scenarios with certain types of uncertainty. For example, if $R_1, \ldots, R_{N_T}$, $K_1, \ldots, K_{N_T}$, and N_0 in (4.5) are confined to linear uncertainty sets as in [40], it can be shown that a robust jammer placement algorithm can be designed based on the minimum possible values of these parameters in the uncertainty sets. Since the structure of the CRLB expressions will not change, all the theoretical results will be valid in that

scenario, as well.[1]

[1]In practice, the jammer node can obtain information about the localization parameters by, e.g., using cameras to learn the locations of the target and anchor nodes, performing prior measurements in the environment to form a database for the channel parameters, and listening to signals between the anchor and target nodes [7].

Bibliography

[1] Z. Sahinoglu, S. Gezici, and I. Guvenc, *Ultra-Wideband Positioning Systems: Theoretical Limits, Ranging Algorithms, and Protocols*. New York, Cambridge University Press, 2008.

[2] R. Zekavat and R. M. Buehrer, *Handbook of Position Location: Theory, Practice and Advances*. John Wiley & Sons, 2011.

[3] S. Gezici, "A survey on wireless position estimation," *Wireless Personal Communications*, vol. 44, pp. 263–282, Feb. 2008.

[4] H. Hu and N. Wei, "A study of GPS jamming and anti-jamming," in *2nd International Conference on Power Electronics and Intelligent Transportation System (PEITS)*, vol. 1, pp. 388–391, Dec. 2009.

[5] D. Lu, R. Wu, and H. Liu, "Global positioning system anti-jamming algorithm based on period repetitive CLEAN," *IET Radar, Sonar & Navigation*, vol. 7, pp. 1640–169, Feb. 2013.

[6] Y. Zhang and M. Amin, "Anti-jamming GPS receiver with reduced phase distortions," *IEEE Signal Process. Lett.*, vol. 19, pp. 635–638, Oct. 2012.

[7] S. Gezici, M. R. Gholami, S. Bayram, and M. Jansson, "Optimal jamming of wireless localization systems," in *IEEE International Conference on Communication Workshop*, pp. 877–882, June 2015.

[8] S. Sankararaman, et. al., "Optimization schemes for protective jamming," in *Proceedings of 13th ACM MobiHoc*, pp. 65–74, June 2012.

[9] A. Shankar, "Optimal jammer placement to interdict wireless network services," *M.S. Thesis*, Naval Postgraduate School, 2008.

[10] J. Zhu and B. Wang, "Sensor placement algorithms for confident information coverage in wireless sensor networks," in *23rd International Conference on Computer Communication and Networks*, Aug. 2014.

[11] W. Li, "Wireless sensor network placement algorithm," in *5th International Conference on Wireless Communications, Networking and Mobile Computing (WiCom)*, Sep. 2009.

[12] L. Ren, Z. Guo, and R. Ma, "Distance-based energy efficient placement in wireless sensor networks," in *3rd IEEE Conference on Industrial Electronics and Applications (ICIEA)*, pp. 2031–2035, June 2008.

[13] E. Biagioni and G. Sasaki, "Wireless sensor placement for reliable and efficient data collection," in *36th Annual Hawaii International Conference on System Sciences*, Jan. 2003.

[14] E. Lloyd and G. Xue, "Relay node placement in wireless sensor networks," *IEEE Transactions on Computers*, vol. 56, pp. 134–138, Jan. 2007.

[15] M. H. E. B. Vadlamani, S. and P. Li, "A bi-level programming model for the wireless network jamming placement problem," in *Industrial and Systems Engineering Research Conference*, 2014.

[16] J. Feng, X. Li, E. Pasiliao, and J. Shea, "Jammer placement to partition wireless network," in *Globecom Workshops*, pp. 1487–1492, Dec. 2014.

[17] K. Grover, A. Lim, and Q. Yang, "Jamming and anti-jamming techniques in wireless networks: A survey," *Int. J. Ad Hoc Ubiquitous Comput.*, vol. 17, pp. 197–215, Dec. 2014.

[18] A. A. Hussein, T. A. Rahman, and C. Y. Leow, "A survey and open issues of jammer localization techniques in wireless sensor networks," *Journal of Theoretical and Applied Information Technology*, vol. 71, pp. 293–301, Jan. 2015.

[19] T. Cheng, P. Li, and S. Zhu, "Multi-jammer localization in wireless sensor networks," in *7th International Conference on Computational Intelligence and Security (CIS)*, pp. 736–740, Dec. 2011.

[20] Y. Sun and X. Wang, "Jammer localization in wireless sensor networks," in *5th International Conference on Wireless Communications, Networking and Mobile Computing (WiCom)*, Sep. 2009.

[21] Z. Liu, H. Liu, W. Xu, and Y. Chen, "Error minimizing jammer localization through smart estimation of ambient noise," in *IEEE 9th International Conference on Mobile Adhoc and Sensor Systems (MASS)*, pp. 308–316, Oct. 2012.

[22] M. Li, I. Koutsopoulos, and R. Poovendran, "Optimal jamming attack strategies and network defense policies in wireless sensor networks," *IEEE Trans. Mobile Comput.*, vol. 9, pp. 1119–1133, Aug. 2010.

[23] A. Houjeij, W. Saad, and T. Bagar, "Optimal deployment of wireless small cell base stations with security considerations," in *IEEE Global Communications Conference (GLOBECOM)*, pp. 607–612, Dec. 2014.

[24] B. Tatham and T. Kunz, "Anchor node placement for localization in wireless sensor networks," in *IEEE 7th International Conference on Wireless and Mobile Computing, Networking and Communications (WiMob)*, pp. 180–187, Oct. 2011.

[25] A. Redondi and E. Amaldi, "Optimizing the placement of anchor nodes in RSS-based indoor localization systems," in *12th Annual Mediterranean Ad Hoc Networking Workshop*, pp. 8–13, June 2013.

[26] R. Akl, K. Pasupathy, and M. Haidar, "Anchor nodes placement for effective passive localization," in *International Conference on Selected Topics in Mobile and Wireless Networking*, pp. 127–132, Oct 2011.

[27] R. Zhang, W. Xia, Z. Jia, L. Shen, and J. Guo, "The optimal placement method of anchor nodes toward RSS-based localization systems," in *Sixth International Conference on Wireless Communications and Signal Processing (WCSP), 2014*, Oct. 2014.

[28] S. Gezici, S. Bayram, M. N. Kurt, and M. R. Gholami, "Optimal jammer placement in wireless localization systems," *IEEE Transactions on Signal Processing*, 2016.

[29] M. K. Simon, J. K. Omura, R. A. Scholtz, and B. K. Levitt, *Spread Spectrum Communications*. Rockville, MD: Comput. Sci. Press, 1985.

[30] M. Weiss and S. C. Schwartz, "On optimal minimax jamming and detection of radar signals," *IEEE Trans. Aeros. Elect. Sys.*, vol. AES-21, pp. 385–393, May 1985.

[31] R. J. McEliece and W. E. Stark, "An information theoretic study of communication in the presence of jamming," in *Int. Conf. Commun. (ICC'81)*, vol. 3, p. 45, 1981.

[32] Y. Shen, W. Dai, and M. Win, "Power optimization for network localization," *IEEE/ACM Trans. Netw.*, vol. 22, pp. 1337–1350, Aug. 2014.

[33] J. Gao, S. A. Vorobyov, H. Jiang, and H. V. Poor, "Worst-case jamming on MIMO Gaussian channels," *IEEE Transactions on Signal Processing*, vol. 63, pp. 5821–5836, Nov. 2015.

[34] G. Amariucai, S. Wei, and R. Kannan, "Gaussian jamming in block-fading channels under long term power constraints," in *IEEE International Symposium on Info. Theory (ISIT)*, pp. 1001–1005, June 2007.

[35] S. N. Diggavi and T. M. Cover, "The worst additive noise under a covariance constraint," *IEEE Trans. Info. Theory*, vol. 47, pp. 3072–3081, Nov. 2001.

[36] R. Bustin, H. V. Poor, and S. Shamai (Shitz), "Worst additive noise: An information-estimation view," in *IEEE 28th Convention of Electrical and Electronics Engineers in Israel*, 2014.

[37] S. M. Kay, *Fundamentals of Statistical Signal Processing: Estimation theory*. Englewood Cliffs, NJ: Prentice-Hall, 1993.

[38] Y. Qi, H. Suda, and H. Kobayashi, "On time-of-arrival positioning in a multipath environment," in *IEEE 60th Vehicular Technology Conference (VTC2004-Fall)*, vol. 5, pp. 3540–3544, Sep. 2004.

[39] Y. Shen and M. Z. Win, "Fundamental limits of wideband localizationpart I: A general framework," *IEEE Transactions on Information Theory*, vol. 56, pp. 4956–4980, Oct. 2010.

[40] W. W.-L. Li, Y. Shen, Y. J. Zhang, and M. Z. Win, "Robust power allocation for energy-efficient location-aware networks," *IEEE/ACM Trans. Netw.*, vol. 21, pp. 1918–1930, Dec. 2013.

[41] T. Wang and G. Leus, "Ranging energy optimization for robust sensor positioning with collaborative anchors," in *IEEE International Conference on Acoustics Speech and Signal Processing (ICASSP)*, pp. 2714–2717, Mar. 2010.

[42] H. V. Poor, *An Introduction to Signal Detection and Estimation*. New York: Springer-Verlag, 1994.

[43] T. Zhang, A. Molisch, Y. Shen, Q. Zhang, and M. Win, "Joint power and bandwidth allocation in cooperative wireless localization networks," in *IEEE Conference on Communications (ICC)*, pp. 2611–2616, June 2014.

[44] A. Goldsmith, *Wireless Communications*. Cambridge University Press, 2005.

[45] D. P. Bertsekas, *Convex Optimization Theory*. Athena Specific, 2009.

[46] P. Biswas and Y. Ye, "Semidefinite programming for ad hoc wireless sensor network localization," in *International Symposium on Information Processing in Sensor Networks (IPSN)*, pp. 46–54, Apr. 2004.

[47] W. Rudin, *Principles of Mathematical Analysis*. Wiley, 3rd ed., 2000.

Appendix A

Proofs and An Auxiliary Result

A.1 Proof of Proposition 1

First, an upper bound is derived for the optimization problem in (4.5) as follows:

$$\max_{\boldsymbol{z}} \min_{i\in\{1,\ldots,N_T\}} R_i\left(\frac{K_iP_J}{\|\boldsymbol{z}-\boldsymbol{x}_i\|^\nu}+\frac{N_0}{2}\right) \leq \max_{\boldsymbol{z}} R_\ell\left(\frac{K_\ell P_J}{\|\boldsymbol{z}-\boldsymbol{x}_\ell\|^\nu}+\frac{N_0}{2}\right) = R_\ell\left(\frac{K_\ell P_J}{\varepsilon^\nu}+\frac{N_0}{2}\right) \tag{A.1}$$

where the inequality follows by definition, and the equality is obtained from the constraint in (4.5). Next, towards the aim of proving the achievability of the upper bound in (A.1) under the conditions in the proposition, the following relation is presented for $i \in \{1,\ldots,N_T\}\setminus\{\ell\}$ and for all $\boldsymbol{z}$ such that $\|\boldsymbol{z}-\boldsymbol{x}_\ell\|=\varepsilon$:

$$R_i\left(\frac{K_iP_J}{\|\boldsymbol{z}-\boldsymbol{x}_i\|^\nu}+\frac{N_0}{2}\right) \geq R_i\left(\frac{K_iP_J}{(\|\boldsymbol{x}_i-\boldsymbol{x}_\ell\|+\varepsilon)^\nu}+\frac{N_0}{2}\right) \geq R_\ell\left(\frac{K_\ell P_J}{\varepsilon^\nu}+\frac{N_0}{2}\right) \tag{A.2}$$

where the first inequality follows from the triangle inequality; that is, $\|\boldsymbol{z}-\boldsymbol{x}_i\| \leq \|\boldsymbol{x}_i-\boldsymbol{x}_\ell\|+\|\boldsymbol{z}-\boldsymbol{x}_\ell\| = \|\boldsymbol{x}_i-\boldsymbol{x}_\ell\|+\varepsilon$, and the second inequality is due to the condition in (4.6). The inequality in (A.2) for $i \in \{1,\ldots,N_T\}\setminus\{\ell\}$ implies that, for $\|\boldsymbol{z}-\boldsymbol{x}_\ell\|=\varepsilon$ and under the condition in (4.6), the upper bound in (A.1) can be achieved as follows: $\min_{i\in\{1,\ldots,N_T\}} R_i\left(\frac{K_iP_J}{\|\boldsymbol{z}-\boldsymbol{x}_i\|^\nu}+\frac{N_0}{2}\right) = R_\ell\left(\frac{K_\ell P_J}{\|\boldsymbol{z}-\boldsymbol{x}_l\|^\nu}+\frac{N_0}{2}\right) =$

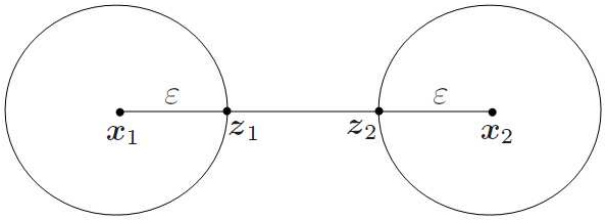

Figure A.1: Illustration of the scenario in Part *(ii)* of Proposition 3.

$R_\ell\left(\frac{K_\ell P_J}{\varepsilon^\nu}+\frac{N_0}{2}\right)$ if set $\{\boldsymbol{z} \,:\, \|\boldsymbol{z}-\boldsymbol{x}_\ell\|=\varepsilon \;\&\; \|\boldsymbol{z}-\boldsymbol{x}_i\|\geq\varepsilon, i=1,\ldots,\ell-1,\ell+1,\ldots,N_T\}$ is non-empty. In other words, under the conditions in the proposition, the optimization problem in (4.5) achieves the upper bound in (A.1) for $\|\boldsymbol{z}-\boldsymbol{x}_\ell\|=\varepsilon$. Hence, the solution $\boldsymbol{z}^{\text{opt}}$ of (4.5) satisfies $\|\boldsymbol{z}^{\text{opt}}-\boldsymbol{x}_\ell\|=\varepsilon$ if the conditions in the proposition hold. ■

A.2 Proof of Proposition 3

(i) If $\|\boldsymbol{x}_1-\boldsymbol{x}_2\|<2\,\varepsilon$, the optimal location for the jammer node, $\boldsymbol{z}^{\text{opt}}$, is equal to one of the two intersection points of the circles centered at $\boldsymbol{x}_1$ and $\boldsymbol{x}_2$ with radii ε. In that case, $\|\boldsymbol{z}^{\text{opt}}-\boldsymbol{x}_1\|=\|\boldsymbol{z}^{\text{opt}}-\boldsymbol{x}_2\|=\varepsilon$ is obtained, which achieves the upper bound of the problem in (4.5) for $N_T=2$. Hence, the solution of (4.5) is given by $\boldsymbol{z}^{\text{opt}}$.

(ii) Suppose that $\|\boldsymbol{x}_1-\boldsymbol{x}_2\|\geq 2\,\varepsilon$. Consider the straight line segment between $\boldsymbol{x}_1$ and $\boldsymbol{x}_2$. Let $\boldsymbol{z}_1$ and $\boldsymbol{z}_2$ denote, respectively, the intersections of this line segment with the circles centered at $\boldsymbol{x}_1$ and $\boldsymbol{x}_2$ with radii ε, as illustrated in Fig. A.1. Denote the straight line segment between $\boldsymbol{z}_1$ and $\boldsymbol{z}_2$ as L_{12}. First, it can be proved that for any feasible location $\boldsymbol{z}^+$ that is not on L_{12}, there exists a location $\boldsymbol{z}^*$ on L_{12} which satisfies either $\|\boldsymbol{z}^*-\boldsymbol{x}_1\|<\|\boldsymbol{z}^+-\boldsymbol{x}_1\|$ & $\|\boldsymbol{z}^*-\boldsymbol{x}_2\|\leq\|\boldsymbol{z}^+-\boldsymbol{x}_2\|$ or $\|\boldsymbol{z}^*-\boldsymbol{x}_1\|\leq\|\boldsymbol{z}^+-\boldsymbol{x}_1\|$ & $\|\boldsymbol{z}^*-\boldsymbol{x}_2\|<\|\boldsymbol{z}^+-\boldsymbol{x}_2\|$. Since, the CRLB is inversely proportional to the distance between the jammer and target nodes, it is concluded that $\boldsymbol{z}^+$ (i.e., any location not on L_{12}) cannot be a solution of (4.5) for $N_T=2$. Hence, the optimal location for the jammer node must satisfy

$\|\boldsymbol{z}^{\rm opt} - \boldsymbol{x}_1\| + \|\boldsymbol{z}^{\rm opt} - \boldsymbol{x}_2\| = \|\boldsymbol{x}_2 - \boldsymbol{x}_1\|$ together with the distance constraints $\|\boldsymbol{z}^{\rm opt} - \boldsymbol{x}_1\| \geq \varepsilon$ and $\|\boldsymbol{z}^{\rm opt} - \boldsymbol{x}_2\| \geq \varepsilon$. In addition, if the condition in (ii)–(a) is satisfied, it means that the CRLB for target node 1 is the minimum CRLB for all $\boldsymbol{z}$ on L_{12}; hence, the optimal solution is to place the jammer node as close to target node 1 as possible in this case; i.e., $\|\boldsymbol{z}^{\rm opt} - \boldsymbol{x}_1\| = \varepsilon$. Similarly, if the condition in (ii)–(b) is satisfied, the CRLB for target node 2 becomes the minimum CRLB for all $\boldsymbol{z}$ on L_{12}, and $\|\boldsymbol{z}^{\rm opt} - \boldsymbol{x}_2\| = \varepsilon$ is obtained. For the condition in (ii)–(c), first suppose that $\|\boldsymbol{z}^{\rm opt} - \boldsymbol{x}_1\| > d^*$, where d^* is as defined in the proposition. In this case, the CRLB for target node 1 becomes the minimum, which is lower than $R_1(K_1 P_J/(d^*)^\nu + N_0/2)$ (see (4.9)). Hence, a contradiction arises, implying that $\|\boldsymbol{z}^{\rm opt} - \boldsymbol{x}_1\| > d^*$ cannot hold. Similarly, in the case of $\|\boldsymbol{z}^{\rm opt} - \boldsymbol{x}_1\| < d^*$, the CRLB for target node 2 becomes the minimum, which is lower than $R_2(K_2 P_J/(\|\boldsymbol{x}_1 - \boldsymbol{x}_2\| - d^*)^\nu + N_0/2)$ (see (4.9)), which leads to a contradiction. Hence, the optimal solution must satisfy $\|\boldsymbol{z}^{\rm opt} - \boldsymbol{x}_1\| = d^*$ under the condition in (ii)–(c). ■

A.3 Proof of Proposition 5

Consider target nodes ℓ_1, ℓ_2, and ℓ_3, and let $\boldsymbol{z}^{\rm opt}_{\ell_1,\ell_2,\ell_3}$ denote the optimizer of (4.14). Also, let $\mathcal{H}$ represent the convex hull formed by the locations of the target nodes, which corresponds to a triangle with the target nodes at the vertices. As stated in the proposition, $\boldsymbol{z}^{\rm opt}_{\ell_1,\ell_2,\ell_3}$ belongs to the interior of $\mathcal{H}$.

First, suppose that the CRLB for one of the target nodes is the minimum and those for the other target nodes are strictly larger for $\boldsymbol{z}^{\rm opt}_{\ell_1,\ell_2,\ell_3}$. Without loss of generality, let ${\rm CRLB}_{\ell_1}(\boldsymbol{z}^{\rm opt}_{\ell_1,\ell_2,\ell_3}) > {\rm CRLB}_{\ell_3}(\boldsymbol{z}^{\rm opt}_{\ell_1,\ell_2,\ell_3})$ and ${\rm CRLB}_{\ell_2}(\boldsymbol{z}^{\rm opt}_{\ell_1,\ell_2,\ell_3}) > {\rm CRLB}_{\ell_3}(\boldsymbol{z}^{\rm opt}_{\ell_1,\ell_2,\ell_3})$. In this case, ${\rm CRLB}_{\ell_1,\ell_2,\ell_3}$ in (4.14) is equal to ${\rm CRLB}_{\ell_3}(\boldsymbol{z}^{\rm opt}_{\ell_1,\ell_2,\ell_3})$. Then, consider the projection of $\boldsymbol{z}^{\rm opt}_{\ell_1,\ell_2,\ell_3}$ onto the straight line that passes through target nodes ℓ_2 and ℓ_3, and denote it by $\boldsymbol{z}_0$. Since $\boldsymbol{z}^{\rm opt}_{\ell_1,\ell_2,\ell_3}$ belongs to the interior of $\mathcal{H}$, there exists $\Delta > 0$ such that $\boldsymbol{z}_\delta \triangleq \boldsymbol{z}^{\rm opt}_{\ell_1,\ell_2,\ell_3} + (\boldsymbol{z}_0 - \boldsymbol{z}^{\rm opt}_{\ell_1,\ell_2,\ell_3})\delta/\|\boldsymbol{z}_0 - \boldsymbol{z}^{\rm opt}_{\ell_1,\ell_2,\ell_3}\|$ belongs to the interior of $\mathcal{H}$ for $\delta \in (0, \Delta)$ (see Fig. A.2-(a) for illustration). For a given value of $\delta \in (0, \Delta)$, $\boldsymbol{z}_\delta$ also corresponds to the projection of $\boldsymbol{z}^{\rm opt}_{\ell_1,\ell_2,\ell_3}$ onto the

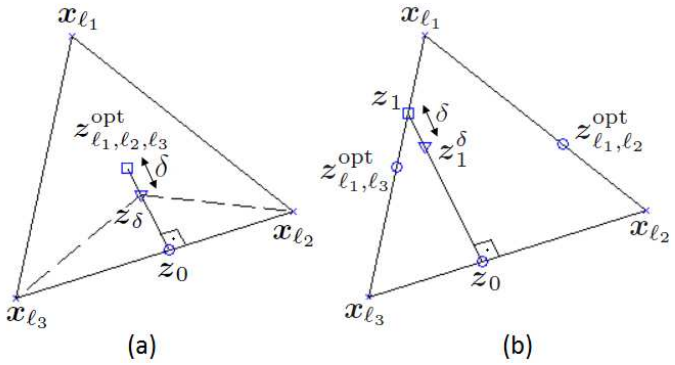

Figure A.2: (a) Illustration for the proof of Proposition 5. (b) Illustration for the proof of Proposition 6.

triangle with vertices at $\boldsymbol{z}_\delta$, $\boldsymbol{x}_{\ell_2}$, and $\boldsymbol{x}_{\ell_3}$. Therefore, based on similar arguments to those in Proposition 4, the projection theorem [45] can be invoked to show that $\boldsymbol{z}_\delta$ is closer to both target node ℓ_2 and target node ℓ_3 than $\boldsymbol{z}^{\text{opt}}_{\ell_1,\ell_2,\ell_3}$; that is,

$$\|\boldsymbol{z}_\delta - \boldsymbol{x}_{\ell_2}\| < \|\boldsymbol{z}^{\text{opt}}_{\ell_1,\ell_2,\ell_3} - \boldsymbol{x}_{\ell_2}\| \tag{A.3}$$

$$\|\boldsymbol{z}_\delta - \boldsymbol{x}_{\ell_3}\| < \|\boldsymbol{z}^{\text{opt}}_{\ell_1,\ell_2,\ell_3} - \boldsymbol{x}_{\ell_3}\| \,. \tag{A.4}$$

Based on Lemma 1 in Appendix A.4, (A.3) and (A.4) implies that

$$\|\boldsymbol{z}_\delta - \boldsymbol{x}_{\ell_1}\| \geq \|\boldsymbol{z}^{\text{opt}}_{\ell_1,\ell_2,\ell_3} - \boldsymbol{x}_{\ell_1}\| \,. \tag{A.5}$$

From (A.3)–(A.5), it is concluded via (4.15) that

$$\text{CRLB}_{\ell_1}(\boldsymbol{z}^{\text{opt}}_{\ell_1,\ell_2,\ell_3}) \geq \text{CRLB}_{\ell_1}(\boldsymbol{z}_\delta) \,, \tag{A.6}$$

$$\text{CRLB}_{\ell_2}(\boldsymbol{z}^{\text{opt}}_{\ell_1,\ell_2,\ell_3}) < \text{CRLB}_{\ell_2}(\boldsymbol{z}_\delta) \,, \tag{A.7}$$

$$\text{CRLB}_{\ell_3}(\boldsymbol{z}^{\text{opt}}_{\ell_1,\ell_2,\ell_3}) < \text{CRLB}_{\ell_3}(\boldsymbol{z}_\delta) \,. \tag{A.8}$$

Since $\text{CRLB}_{\ell_1}(\boldsymbol{z}^{\text{opt}}_{\ell_1,\ell_2,\ell_3}) > \text{CRLB}_{\ell_3}(\boldsymbol{z}^{\text{opt}}_{\ell_1,\ell_2,\ell_3})$ and the CRLB in (4.15) is a continuous function of the distance, there exists $\delta \in (0, \Delta)$ such that

$$\text{CRLB}_{\ell_1}(\boldsymbol{z}_\delta) > \text{CRLB}_{\ell_3}(\boldsymbol{z}^{\text{opt}}_{\ell_1,\ell_2,\ell_3}) = \text{CRLB}_{\ell_1,\ell_2,\ell_3}(\boldsymbol{z}^{\text{opt}}_{\ell_1,\ell_2,\ell_3}) \,. \tag{A.9}$$

The relations in (A.6)–(A.9) together with $\text{CRLB}_{\ell_1}(\boldsymbol{z}^{\text{opt}}_{\ell_1,\ell_2,\ell_3}) > \text{CRLB}_{\ell_3}(\boldsymbol{z}^{\text{opt}}_{\ell_1,\ell_2,\ell_3})$ and $\text{CRLB}_{\ell_2}(\boldsymbol{z}^{\text{opt}}_{\ell_1,\ell_2,\ell_3}) > \text{CRLB}_{\ell_3}(\boldsymbol{z}^{\text{opt}}_{\ell_1,\ell_2,\ell_3})$ imply that there exists $\delta \in (0, \Delta)$ such that $\text{CRLB}_{\ell_1,\ell_2,\ell_3}(\boldsymbol{z}_\delta) > \text{CRLB}_{\ell_1,\ell_2,\ell_3}(\boldsymbol{z}^{\text{opt}}_{\ell_1,\ell_2,\ell_3})$. Therefore, $\boldsymbol{z}^{\text{opt}}_{\ell_1,\ell_2,\ell_3}$ is not optimal,

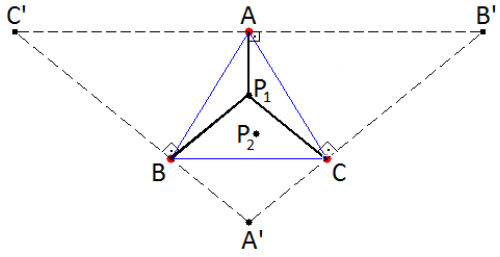

Figure A.3: Illustration for the proof of Lemma 1.

which leads to a contradiction. Hence, it is not possible that the CRLB for one of the target nodes is the minimum and those for the other target nodes are strictly larger for $\boldsymbol{z}^{\text{opt}}_{\ell_1,\ell_2,\ell_3}$.

Secondly, suppose that two of the CRLBs for the target nodes are the same and that for the other target node is larger. Without loss of generality, let $\text{CRLB}_{\ell_1}(\boldsymbol{z}^{\text{opt}}_{\ell_1,\ell_2,\ell_3}) > \text{CRLB}_{\ell_2}(\boldsymbol{z}^{\text{opt}}_{\ell_1,\ell_2,\ell_3}) = \text{CRLB}_{\ell_3}(\boldsymbol{z}^{\text{opt}}_{\ell_1,\ell_2,\ell_3})$. Based on the same arguments as in the previous case, it can be shown that there exists $\boldsymbol{z}_\delta$ for which the relations in (A.6)–(A.9) hold. Therefore, $\text{CRLB}_{\ell_1,\ell_2,\ell_3}(\boldsymbol{z}_\delta) > \text{CRLB}_{\ell_1,\ell_2,\ell_3}(\boldsymbol{z}^{\text{opt}}_{\ell_1,\ell_2,\ell_3})$ is obtained, resulting in a contradiction. Hence, the only feasible scenario in which $\boldsymbol{z}^{\text{opt}}_{\ell_1,\ell_2,\ell_3}$ belongs to the interior of $\mathcal{H}$ is the one with $\text{CRLB}_{\ell_1}(\boldsymbol{z}^{\text{opt}}_{\ell_1,\ell_2,\ell_3}) = \text{CRLB}_{\ell_2}(\boldsymbol{z}^{\text{opt}}_{\ell_1,\ell_2,\ell_3}) = \text{CRLB}_{\ell_3}(\boldsymbol{z}^{\text{opt}}_{\ell_1,\ell_2,\ell_3})$. ■

A.4 An Auxiliary Result

Lemma 1: *Consider a triangle in a two-dimensional space with vertices A, B, and C, and a point P_1 inside the triangle. Let $d_{A,1}$, $d_{B,1}$, and $d_{C,1}$ denote the distances of P_1 from vertices A, B, and C, respectively. Consider another point P_2 on the triangle with distances $d_{A,2}$, $d_{B,2}$, and $d_{C,2}$ from vertices A, B, and C, respectively. If $d_{B,2} \leq d_{B,1}$ and $d_{C,2} \leq d_{C,1}$, then $d_{A,2} \geq d_{A,1}$.*

Proof. Consider a triangle with vertices A, B, and C, and two points P_1 and P_2 as shown in Fig. A.3. First, a new triangle with vertices A', B', and C' is formed as shown in the figure, where the edges of the triangle are the straight lines which

pass through A, B, and C, and are perpendicular to the straight lines from point P_1 to the vertices of triangle ABC. Since P_1 belongs to the interior of triangle ABC, the edges $A'B'$, $B'C'$, and $A'C'$ are guaranteed to form a triangle (i.e., they cannot be parallel to each other). The area of triangle $A'B'C'$ is given by

$$\text{Area}(A'B'C') = \frac{d_{C,1}|A'B'| + d_{B,1}|A'C'| + d_{A,1}|B'C'|}{2} \tag{A.10}$$

where $d_{A,1}$, $d_{B,1}$, and $d_{C,1}$ are the distances between point P_1 and vertices A, B, and C, respectively, and $|A'B'|$, $|A'C'|$, and $|B'C'|$ denote the lengths of the edges between vertices A' and B', A' and C', and B' and C', respectively. The same area can also be calculated as

$$\text{Area}(A'B'C') = \frac{h'_C|A'B'| + h'_B|A'C'| + h'_A|B'C'|}{2} \tag{A.11}$$

where h'_A, h'_B, and h'_C are the distances between point P_2 and edges $B'C'$, $A'C'$, and $A'B'$, respectively. From the definition of distance between a point and a straight line, the following relations are obtained:

$$h'_A \leq d_{A,2}\,,\ h'_B \leq d_{B,2}\,,\ h'_C \leq d_{C,2} \tag{A.12}$$

where $d_{A,2}$, $d_{B,2}$ and $d_{C,2}$ are the distances between point P_2 and vertices A, B and C, respectively. Suppose that $d_{B,2} \leq d_{B,1}$ and $d_{C,2} \leq d_{C,1}$, as stated in the lemma. Then, from (A.12), $h'_B \leq d_{B,1}$ and $h'_C \leq d_{C,1}$ hold, which imply that for the equality of the area expressions in (A.10) and (A.11), $d_{A,1} \leq h'_A$ must be satisfied. Hence, $d_{A,1} \leq d_{A,2}$ must hold due to (A.12). □

A.5 Proof of Proposition 6

Part a): Consider the scenario in which the optimal jammer location is on the boundary of the triangle formed by target nodes ℓ_1, ℓ_2, and ℓ_3. First, suppose that $\boldsymbol{z}_1$ is an optimal location for the jammer node, which lies on the straight line segment between $\boldsymbol{x}_{\ell_1}$ and $\boldsymbol{z}^{\text{opt}}_{\ell_1,\ell_3}$, where $\boldsymbol{x}_{\ell_1}$ is the location of target node ℓ_1 and $\boldsymbol{z}^{\text{opt}}_{\ell_1,\ell_3}$ is the optimizer of (4.16) for target nodes ℓ_1 and ℓ_3, which corresponds to $\text{CRLB}_{\ell_1,\ell_3}$. As stated in the proposition, $\text{CRLB}_{\ell_1,\ell_2} < \text{CRLB}_{\ell_1,\ell_3}$. Therefore, due

to the equalizer property in Corollary 1, $\mathrm{CRLB}_{\ell_1}(\boldsymbol{z}^{\mathrm{opt}}_{\ell_1,\ell_2}) < \mathrm{CRLB}_{\ell_1}(\boldsymbol{z}^{\mathrm{opt}}_{\ell_1,\ell_3})$ must hold. Then, the following relations are obtained:

$$\|\boldsymbol{x}_{\ell_1} - \boldsymbol{z}^{\mathrm{opt}}_{\ell_1,\ell_2}\| > \|\boldsymbol{x}_{\ell_1} - \boldsymbol{z}^{\mathrm{opt}}_{\ell_1,\ell_3}\| \geq \|\boldsymbol{x}_{\ell_1} - \boldsymbol{z}_1\| \tag{A.13}$$

where the first inequality follows from $\mathrm{CRLB}_{\ell_1}(\boldsymbol{z}^{\mathrm{opt}}_{\ell_1,\ell_2}) < \mathrm{CRLB}_{\ell_1}(\boldsymbol{z}^{\mathrm{opt}}_{\ell_1,\ell_3})$ and (4.15), and the second inequality is by the definition of location $\boldsymbol{z}_1$ (see Fig. A.2-(b) for illustration). The inequality in (A.13) and the equalizer property in Corollary 1 imply that

$$\mathrm{CRLB}_{\ell_1}(\boldsymbol{z}_1) > \mathrm{CRLB}_{\ell_1}(\boldsymbol{z}^{\mathrm{opt}}_{\ell_1,\ell_2}) = \mathrm{CRLB}_{\ell_1,\ell_2}\,. \tag{A.14}$$

On the other hand, due to the definitions in (4.14) and (4.16), the following relation always holds:

$$\mathrm{CRLB}_{\ell_1,\ell_2,\ell_3} \leq \mathrm{CRLB}_{\ell_1,\ell_2}\,. \tag{A.15}$$

Since $\boldsymbol{z}_1$ is an optimal solution of (4.14), $\mathrm{CRLB}_{\ell_1,\ell_2,\ell_3}$ is equal to $\min\{\mathrm{CRLB}_{\ell_1}(\boldsymbol{z}_1), \mathrm{CRLB}_{\ell_2}(\boldsymbol{z}_1), \mathrm{CRLB}_{\ell_3}(\boldsymbol{z}_1)\}$, which, together with (A.14) and (A.15), imply that $\mathrm{CRLB}_{\ell_1}(\boldsymbol{z}_1)$ is not a minimum of $\{\mathrm{CRLB}_{\ell_1}(\boldsymbol{z}_1), \mathrm{CRLB}_{\ell_2}(\boldsymbol{z}_1), \mathrm{CRLB}_{\ell_3}(\boldsymbol{z}_1)\}$. Then, a new location $\boldsymbol{z}_1^{\delta}$ is defined, which is at distance of $\delta > 0$ from $\boldsymbol{z}_1$ and is on the straight line segment between $\boldsymbol{z}_1$ and the projection of $\boldsymbol{z}_1$ on the straight line that passes through $\boldsymbol{x}_{\ell_2}$ and $\boldsymbol{x}_{\ell_3}$, as shown in Fig. A.2-(b).[1] Since the distance between $\boldsymbol{z}_1^{\delta}$ and $\boldsymbol{x}_{\ell_2}$ ($\boldsymbol{x}_{\ell_3}$) is smaller than the distance between $\boldsymbol{z}_1$ and $\boldsymbol{x}_{\ell_2}$ ($\boldsymbol{x}_{\ell_3}$) (based on the projection theorem [45] and similar arguments to those in the proof of Proposition 4), the following relations are obtained from (4.15):

$$\mathrm{CRLB}_{\ell_2}(\boldsymbol{z}_1^{\delta}) > \mathrm{CRLB}_{\ell_2}(\boldsymbol{z}_1) \tag{A.16}$$

$$\mathrm{CRLB}_{\ell_3}(\boldsymbol{z}_1^{\delta}) > \mathrm{CRLB}_{\ell_3}(\boldsymbol{z}_1) \tag{A.17}$$

In addition, since the CRLB is a continuous function of the distance, there always exists a sufficiently small $\delta > 0$ such that $\mathrm{CRLB}_{\ell_1}(\boldsymbol{z}_1^{\delta}) > \mathrm{CRLB}_{\ell_1,\ell_2}$ (see (A.14)). Hence, based on similar arguments to those above, $\mathrm{CRLB}_{\ell_1}(\boldsymbol{z}_1^{\delta})$ is not

[1] Note that $\boldsymbol{z}_1^{\delta}$ is not required to be on the triangle formed by the locations of the target nodes; it may also be outside that triangle.

the minimum of $\{\mathrm{CRLB}_{\ell_1}(\boldsymbol{z}_1^\delta), \mathrm{CRLB}_{\ell_2}(\boldsymbol{z}_1^\delta), \mathrm{CRLB}_{\ell_3}(\boldsymbol{z}_1^\delta)\}$. Therefore, based on (A.16) and (A.17), it is concluded that

$$\begin{aligned}\min\{\mathrm{CRLB}_{\ell_1}(\boldsymbol{z}_1^\delta), \mathrm{CRLB}_{\ell_2}(\boldsymbol{z}_1^\delta), \mathrm{CRLB}_{\ell_3}(\boldsymbol{z}_1^\delta)\} > \\ \min\{\mathrm{CRLB}_{\ell_1}(\boldsymbol{z}_1), \mathrm{CRLB}_{\ell_2}(\boldsymbol{z}_1), \mathrm{CRLB}_{\ell_3}(\boldsymbol{z}_1)\}\end{aligned} \tag{A.18}$$

which contradicts the optimality of $\boldsymbol{z}_1$. Hence, it is proved via contradiction that no locations on the straight line segment between $\boldsymbol{x}_{\ell_1}$ and $\boldsymbol{z}_{\ell_1,\ell_3}^{\mathrm{opt}}$ can be optimal.

Secondly, suppose that $\boldsymbol{z}_2$ is an optimal location for the jammer node, which lies on the straight line segment between $\boldsymbol{x}_{\ell_3}$ and $\boldsymbol{z}_{\ell_1,\ell_3}^{\mathrm{opt}}$, where $\boldsymbol{z}_{\ell_1,\ell_3}^{\mathrm{opt}}$ is the optimizer of (4.16) for target nodes ℓ_1 and ℓ_3, corresponding to $\mathrm{CRLB}_{\ell_1,\ell_3}$. Let the upper bound in (4.17) be denoted by d_{thr}. Then, it is obtained that

$$\mathrm{CRLB}_{\ell_1,\ell_2} = R_{\ell_3}\left(K_{\ell_3} P_J / d_{\mathrm{thr}}^{\nu} + N_0/2\right) . \tag{A.19}$$

Since $\mathrm{CRLB}_{\ell_1,\ell_2} < \mathrm{CRLB}_{\ell_1,\ell_3}$ as stated in the proposition, the equalizer property in Corollary 1 implies that $\mathrm{CRLB}_{\ell_1,\ell_2} < \mathrm{CRLB}_{\ell_1}(\boldsymbol{z}_{\ell_1,\ell_3}^{\mathrm{opt}})$, which, via (4.15) and (A.19), leads to

$$d_{\mathrm{thr}} > \|\boldsymbol{x}_{\ell_3} - \boldsymbol{z}_{\ell_1,\ell_3}^{\mathrm{opt}}\| \geq \|\boldsymbol{x}_{\ell_3} - \boldsymbol{z}_2\| \tag{A.20}$$

where the last inequality follows from the definition of $\boldsymbol{z}_2$. From (A.19) and (A.20), it is obtained that $\mathrm{CRLB}_{\ell_3}(\boldsymbol{z}_2) > \mathrm{CRLB}_{\ell_1,\ell_2}$. Since $\min\{\mathrm{CRLB}_{\ell_1}(\boldsymbol{z}_2), \mathrm{CRLB}_{\ell_2}(\boldsymbol{z}_2), \mathrm{CRLB}_{\ell_3}(\boldsymbol{z}_2)\}$ is upper bounded by $\mathrm{CRLB}_{\ell_1,\ell_2}$ by definition (see (4.14) and (4.16)), it can be concluded from the relation $\mathrm{CRLB}_{\ell_3}(\boldsymbol{z}_2) > \mathrm{CRLB}_{\ell_1,\ell_2}$ that $\mathrm{CRLB}_{\ell_3}(\boldsymbol{z}_2)$ is not a minimum of $\{\mathrm{CRLB}_{\ell_1}(\boldsymbol{z}_2), \mathrm{CRLB}_{\ell_2}(\boldsymbol{z}_2), \mathrm{CRLB}_{\ell_3}(\boldsymbol{z}_2)\}$. Then, a new location $\boldsymbol{z}_2^\delta$ can be defined as in the first case, and it can be shown that $\boldsymbol{z}_2$ cannot be optimal (cf. (A.16)–(A.18)).

Based on similar arguments to those in the two cases above, it can be shown that no locations on the straight line between $\boldsymbol{x}_{\ell_2}$ and $\boldsymbol{x}_{\ell_3}$ can be optimal.

Next, suppose that $\boldsymbol{z}_3$ is an optimal location for the jammer node, which lies on the straight line segment between $\boldsymbol{x}_{\ell_1}$ and $\boldsymbol{z}_{\ell_1,\ell_2}^{\mathrm{opt}}$ (excluding $\boldsymbol{z}_{\ell_1,\ell_2}^{\mathrm{opt}}$), where $\boldsymbol{z}_{\ell_1,\ell_2}^{\mathrm{opt}}$ is

the optimizer of (4.16) for target nodes ℓ_1 and ℓ_2, which corresponds to $\mathrm{CRLB}_{\ell_1,\ell_2}$. Since $\|\boldsymbol{x}_{\ell_1} - \boldsymbol{z}_{\ell_1,\ell_2}^{\mathrm{opt}}\| > \|\boldsymbol{x}_{\ell_1} - \boldsymbol{z}_3\|$, it is obtained that

$$\mathrm{CRLB}_{\ell_1}(\boldsymbol{z}_3) > \mathrm{CRLB}_{\ell_1}(\boldsymbol{z}_{\ell_1,\ell_2}^{\mathrm{opt}}) = \mathrm{CRLB}_{\ell_1,\ell_2} \tag{A.21}$$

where the equality is due to Corollary 1. Based on similar arguments to those in the first two cases, (A.21) implies that $\mathrm{CRLB}_{\ell_3}(\boldsymbol{z}_3)$ is not a minimum of $\{\mathrm{CRLB}_{\ell_1}(\boldsymbol{z}_3), \mathrm{CRLB}_{\ell_2}(\boldsymbol{z}_3), \mathrm{CRLB}_{\ell_3}(\boldsymbol{z}_3)\}$. Then, a new location $\boldsymbol{z}_3^{\delta}$ can be defined as in the first case, and it can be shown that $\boldsymbol{z}_3$ cannot be optimal (cf. (A.16)–(A.18)).

Finally, if $\boldsymbol{z}_4$ is an optimal location for the jammer node, which lies on the straight line segment between $\boldsymbol{x}_{\ell_2}$ and $\boldsymbol{z}_{\ell_1,\ell_2}^{\mathrm{opt}}$ (excluding $\boldsymbol{z}_{\ell_1,\ell_2}^{\mathrm{opt}}$), it can be shown in a similar manner to the previous case that $\boldsymbol{z}_4$ cannot be optimal.

Overall, the only possible location on the boundary of the convex hull (triangle) is $\boldsymbol{z}_{\ell_1,\ell_2}^{\mathrm{opt}}$ for which $\mathrm{CRLB}_{\ell_1}(\boldsymbol{z}_{\ell_1,\ell_2}^{\mathrm{opt}}) = \mathrm{CRLB}_{\ell_2}(\boldsymbol{z}_{\ell_1,\ell_2}^{\mathrm{opt}})$ due to Corollary 1. Hence, if the optimal jammer location is on the boundary of the triangle formed by target nodes ℓ_1, ℓ_2, and ℓ_3, then the optimizer of (4.14) is equal to $\boldsymbol{z}_{\ell_1,\ell_2}^{\mathrm{opt}}$.

Part b): If the condition in (4.17) holds, it then follows form (4.15) that $\mathrm{CRLB}_{\ell_3}(\boldsymbol{z}_{\ell_1,\ell_2}^{\mathrm{opt}}) \geq \mathrm{CRLB}_{\ell_1,\ell_2}$. Then, Proposition 2 can be invoked to conclude that $\boldsymbol{z}_{\ell_1,\ell_2}^{\mathrm{opt}}$ is the optimal jammer location corresponding to (4.14). Hence, the optimal location for the jammer node is on the boundary of the convex hull (triangle) formed by the target nodes. To prove the necessity of (4.17), suppose that the optimal jammer location is on the boundary of the triangle. Then, the proof of Part a) shows that the optimal location for the jammer node is $\boldsymbol{z}_{\ell_1,\ell_2}^{\mathrm{opt}}$, which achieves a CRLB denoted by $\mathrm{CRLB}_{\ell_1,\ell_2}$. Due to the formulation in (4.14), $\mathrm{CRLB}_{\ell_1,\ell_2}$ is equal to $\min\{\mathrm{CRLB}_{\ell_1}(\boldsymbol{z}_{\ell_1,\ell_2}^{\mathrm{opt}}), \mathrm{CRLB}_{\ell_2}(\boldsymbol{z}_{\ell_1,\ell_2}^{\mathrm{opt}}), \mathrm{CRLB}_{\ell_3}(\boldsymbol{z}_{\ell_1,\ell_2}^{\mathrm{opt}})\}$ in this scenario. Hence, $\mathrm{CRLB}_{\ell_3}(\boldsymbol{z}_{\ell_1,\ell_2}^{\mathrm{opt}}) \geq \mathrm{CRLB}_{\ell_1,\ell_2}$ must hold, which, based on (4.15), leads to (4.17). ■

A.6 Proof of Proposition 7

Consider the optimal jammer placement problem in (4.5) in the absence of distance constraints:

$$\max_{\boldsymbol{z}} \min_{m\in\{1,\ldots,N_T\}} \mathrm{CRLB}_m(\boldsymbol{z}) \tag{A.22}$$

where $\mathrm{CRLB}_m(\boldsymbol{z})$ is as in (4.15). The aim is to prove that the optimizer of (A.22) and the corresponding optimal value are equal to $\boldsymbol{z}_{i,j,k}^{\mathrm{opt}}$ and $\mathrm{CRLB}_{i,j,k}$, respectively, which are as defined in the proposition. Based on Proposition 4, $\boldsymbol{z}_{i,j,k}^{\mathrm{opt}}$ lies on the convex hull (triangle in this case) formed by the locations of target nodes i, j, and k.

Case 1: First, assume that $\boldsymbol{z}_{i,j,k}^{\mathrm{opt}}$ belongs to the *interior* of the triangle formed by these target nodes. Then, from Proposition 5, the max-min solution in (4.14) for target nodes i, j, and k equalizes the CRLBs of these target nodes; that is, $\mathrm{CRLB}_i(\boldsymbol{z}_{i,j,k}^{\mathrm{opt}}) = \mathrm{CRLB}_j(\boldsymbol{z}_{i,j,k}^{\mathrm{opt}}) = \mathrm{CRLB}_k(\boldsymbol{z}_{i,j,k}^{\mathrm{opt}}) = \mathrm{CRLB}_{i,j,k}$. Next, consider target node ℓ^*, which is different from target nodes i, j, and k. Since all the targets are on the two dimensional space, $\boldsymbol{z}_{i,j,k}^{\mathrm{opt}}$ must be on one of the triangles formed by target node ℓ^* and any two of target nodes i, j, and k. Without loss of generality, let that triangle be formed by target nodes ℓ^*, i and j (see Fig. A.4), and let the max-min solution in (4.14) for these three target nodes be denoted by $\mathrm{CRLB}_{i,j,\ell^*}$ with the corresponding optimizer of $\boldsymbol{z}_{i,j,\ell^*}^{\mathrm{opt}}$. Since $\mathrm{CRLB}_{i,j,\ell^*} \geq \mathrm{CRLB}_{i,j,k}$ by definition, $\mathrm{CRLB}_{i,j,\ell^*} = \min\{\mathrm{CRLB}_i(\boldsymbol{z}_{i,j,\ell^*}^{\mathrm{opt}}), \mathrm{CRLB}_j(\boldsymbol{z}_{i,j,\ell^*}^{\mathrm{opt}}), \mathrm{CRLB}_{\ell^*}(\boldsymbol{z}_{i,j,\ell^*}^{\mathrm{opt}})\} \geq \mathrm{CRLB}_{i,j,k} = \mathrm{CRLB}_i(\boldsymbol{z}_{i,j,k}^{\mathrm{opt}}) = \mathrm{CRLB}_j(\boldsymbol{z}_{i,j,k}^{\mathrm{opt}}) = \mathrm{CRLB}_k(\boldsymbol{z}_{i,j,k}^{\mathrm{opt}})$ must hold. Therefore, $\mathrm{CRLB}_i(\boldsymbol{z}_{i,j,\ell^*}^{\mathrm{opt}}) \geq \mathrm{CRLB}_i(\boldsymbol{z}_{i,j,k}^{\mathrm{opt}})$ and $\mathrm{CRLB}_j(\boldsymbol{z}_{i,j,\ell^*}^{\mathrm{opt}}) \geq \mathrm{CRLB}_j(\boldsymbol{z}_{i,j,k}^{\mathrm{opt}})$ are obtained, which imply that (cf. (4.15))

$$\|\boldsymbol{x}_i - \boldsymbol{z}_{i,j,\ell^*}^{\mathrm{opt}}\| \leq \|\boldsymbol{x}_i - \boldsymbol{z}_{i,j,k}^{\mathrm{opt}}\|,\ \|\boldsymbol{x}_j - \boldsymbol{z}_{i,j,\ell^*}^{\mathrm{opt}}\| \leq \|\boldsymbol{x}_j - \boldsymbol{z}_{i,j,k}^{\mathrm{opt}}\|. \tag{A.23}$$

Next, consider the two possible cases for $\boldsymbol{z}_{i,j,k}^{\mathrm{opt}}$:

Case 1-(a): In this case, $\boldsymbol{z}_{i,j,k}^{\mathrm{opt}}$ belongs to the *interior* of the triangle formed by target nodes i, j, and ℓ^*, as shown in Fig. A.4-(a). Then, by Lemma 1 (see

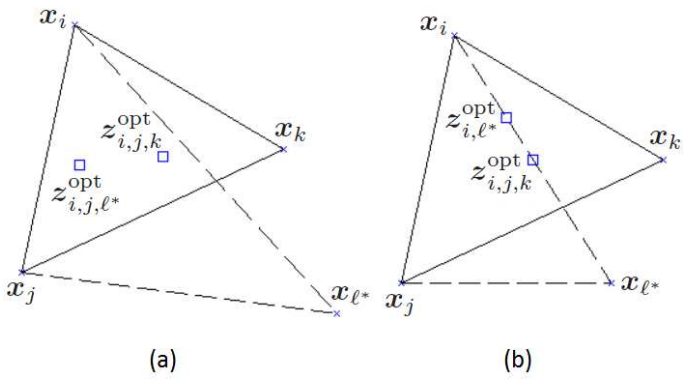

Figure A.4: Illustration for Case 1 of the proof of Proposition 7: (a) Case 1-(a), (b) Case 1-(b).

Appendix A.4), it follows from (A.23) that

$$\|\boldsymbol{x}_{\ell^*} - \boldsymbol{z}^{\text{opt}}_{i,j,k}\| \leq \|\boldsymbol{x}_{\ell^*} - \boldsymbol{z}^{\text{opt}}_{i,j,\ell^*}\| \tag{A.24}$$

which implies $\text{CRLB}_{\ell^*}(\boldsymbol{z}^{\text{opt}}_{i,j,k}) \geq \text{CRLB}_{\ell^*}(\boldsymbol{z}^{\text{opt}}_{i,j,\ell^*})$; hence, the following relation is obtained:

$$\text{CRLB}_{\ell^*}(\boldsymbol{z}^{\text{opt}}_{i,j,k}) \geq \text{CRLB}_{\ell^*}(\boldsymbol{z}^{\text{opt}}_{i,j,\ell^*}) \geq \text{CRLB}_{i,j,\ell^*} \geq \text{CRLB}_{i,j,k} \tag{A.25}$$

where the second inequality follows from (4.14) and the third inequality is due to the assumption in the proposition. The inequality in (A.25) indicates that the optimal jammer location $\boldsymbol{z}^{\text{opt}}_{i,j,k}$ obtained by considering target nodes i, j, and k only results in a larger CRLB for target node ℓ^* than $\text{CRLB}_{i,j,k}$, where ℓ^* is an arbitrary target node with $\ell^* \notin \{i, j, k\}$. Therefore, for the jammer node location $\boldsymbol{z}^{\text{opt}}_{i,j,k}$, the objective function in (A.22) becomes

$$\min_{m \in \{1,\ldots,N_T\}} \text{CRLB}_m(\boldsymbol{z}^{\text{opt}}_{i,j,k}) = \text{CRLB}_{i,j,k}\,. \tag{A.26}$$

Since $\text{CRLB}_{i,j,k}$ is an upper bound on (A.22) (since only three target nodes are considered in (4.14)), which is achieved for $\boldsymbol{z}^{\text{opt}}_{i,j,k}$ as specified in (A.26), the solution of (A.22) is given by $\boldsymbol{z}^{\text{opt}}_{i,j,k}$ under the conditions in the proposition.

Case 1-(b): In this case, $\boldsymbol{z}^{\text{opt}}_{i,j,k}$ is on the edge of the triangle connecting target nodes i and ℓ^*, as shown in Fig. A.4-(b). (The same arguments below apply to the case in which $\boldsymbol{z}^{\text{opt}}_{i,j,k}$ is on the edge of the triangle connecting target nodes

j and ℓ^*.) Then, it is first obtained that $\mathrm{CRLB}_{i,\ell^*} \geq \mathrm{CRLB}_{i,j,\ell^*} \geq \mathrm{CRLB}_{i,j,k}$, where CRLB_{i,ℓ^*} denotes the solution of (4.16) for target nodes i and ℓ^*. Let $\boldsymbol{z}_{i,\ell^*}^{\mathrm{opt}}$ denote the optimizer of (4.16) that results in CRLB_{i,ℓ^*}. Due to the equalizer solutions corresponding to CRLB_{i,ℓ^*} and $\mathrm{CRLB}_{i,j,k}$ (see Corollary 1 and Proposition 5), $\mathrm{CRLB}_{i,\ell^*} \geq \mathrm{CRLB}_{i,j,k}$ implies that $\mathrm{CRLB}_i(\boldsymbol{z}_{i,\ell^*}^{\mathrm{opt}}) \geq \mathrm{CRLB}_i(\boldsymbol{z}_{i,j,k}^{\mathrm{opt}})$. Hence, the distance between $\boldsymbol{z}_{i,\ell^*}^{\mathrm{opt}}$ and target node i is smaller than or equal to the distance between $\boldsymbol{z}_{i,j,k}^{\mathrm{opt}}$ and target node i. Since both $\boldsymbol{z}_{i,\ell^*}^{\mathrm{opt}}$ and $\boldsymbol{z}_{i,j,k}^{\mathrm{opt}}$ are on the straight line segment connecting target nodes i and ℓ^*, the following distance relation is obtained: $\|\boldsymbol{x}_{\ell^*} - \boldsymbol{z}_{i,j,k}^{\mathrm{opt}}\| \leq \|\boldsymbol{x}_{\ell^*} - \boldsymbol{z}_{i,\ell^*}^{\mathrm{opt}}\|$, which leads to $\mathrm{CRLB}_{\ell^*}(\boldsymbol{z}_{i,j,k}^{\mathrm{opt}}) \geq \mathrm{CRLB}_{\ell^*}(\boldsymbol{z}_{i,\ell^*}^{\mathrm{opt}})$; hence, it follows that

$$\mathrm{CRLB}_{\ell^*}(\boldsymbol{z}_{i,j,k}^{\mathrm{opt}}) \geq \mathrm{CRLB}_{\ell^*}(\boldsymbol{z}_{i,\ell^*}^{\mathrm{opt}}) \geq \mathrm{CRLB}_{i,\ell^*} \geq \mathrm{CRLB}_{i,j,\ell^*} \geq \mathrm{CRLB}_{i,j,k}\,. \quad \text{(A.27)}$$

Then, arguments similar to those in Case 1-(a) can be employed to prove that the solution of (A.22) is given by $\boldsymbol{z}_{i,j,k}^{\mathrm{opt}}$ in this case, as well.

Case 2: Secondly, consider the case in which $\boldsymbol{z}_{i,j,k}^{\mathrm{opt}}$ is on the *boundary* of the triangle formed by target nodes i, j, and k. Let $\boldsymbol{z}_{i,j,k}^{\mathrm{opt}}$ be on the straight line connecting target nodes i and j without loss of generality. Then, from Proposition 6, the jammer location $\boldsymbol{z}_{i,j,k}^{\mathrm{opt}}$ equalizes the CRLBs for target nodes i and j, and is given by the optimal solution of (4.16) corresponding to target nodes i and j; that is, $\boldsymbol{z}_{i,j,k}^{\mathrm{opt}} = \boldsymbol{z}_{i,j}^{\mathrm{opt}}$ and $\mathrm{CRLB}_{i,j,k} = \mathrm{CRLB}_{i,j}$. Since the network consisting of the target nodes i and j is a subnetwork of the network consisting of the target nodes i, j, and ℓ^*, the following relation holds: $\mathrm{CRLB}_{i,j,\ell^*} \leq \mathrm{CRLB}_{i,j}$. On the other hand, since $\mathrm{CRLB}_{i,j,k} \leq \mathrm{CRLB}_{i,j,\ell^*}$ by definition, $\mathrm{CRLB}_{i,j} \leq \mathrm{CRLB}_{i,j,\ell^*}$ must also hold. Therefore, $\mathrm{CRLB}_{i,j} = \mathrm{CRLB}_{i,j,\ell^*}$ in this case, and it can shown that $\boldsymbol{z}_{i,j}^{\mathrm{opt}} = \boldsymbol{z}_{\ell^*,i,j}^{\mathrm{opt}}$ is the only possibility. Then, based on similar arguments to those in Case 1, it can be shown that target node ℓ^* has no effect on the optimal solution for all $\ell^* \notin \{i,j,k\}$; i.e., the solution of (A.22) is given by $\boldsymbol{z}_{i,j,k}^{\mathrm{opt}} = \boldsymbol{z}_{i,j}^{\mathrm{opt}}$ under the conditions in the proposition. ■

A.7 Proof of Corollary 2

Since $\boldsymbol{z}_{i,j,k}^{\text{opt}}$, belongs to the interior of the convex hull formed by target nodes i, j, and k, Proposition 5 implies that $\text{CRLB}_{i,j,k} = \text{CRLB}_i(\boldsymbol{z}_{i,j,k}^{\text{opt}}) = \text{CRLB}_j(\boldsymbol{z}_{i,j,k}^{\text{opt}}) = \text{CRLB}_k(\boldsymbol{z}_{i,j,k}^{\text{opt}})$. In addition, $\text{CRLB}_{i,j,k} \leq \text{CRLB}_{i,j} = \text{CRLB}_i(\boldsymbol{z}_{i,j}^{\text{opt}}) = \text{CRLB}_j(\boldsymbol{z}_{i,j}^{\text{opt}})$ always holds due to (4.14), (4.16), and Corollary 1. If $\boldsymbol{z}_{i,j,k}^{\text{opt}}$ is inside the circle centered at target node i with radius $\|\boldsymbol{x}_i - \boldsymbol{z}_{i,j}^{\text{opt}}\|$, it implies that $\text{CRLB}_i(\boldsymbol{z}_{i,j,k}^{\text{opt}}) > \text{CRLB}_i(\boldsymbol{z}_{i,j}^{\text{opt}}) = \text{CRLB}_{i,j} \geq \text{CRLB}_{i,j,k}$, which results in a contradiction (c.f. the first sentence of the proof). Similarly, if $\boldsymbol{z}_{i,j,k}^{\text{opt}}$ is inside the circle centered at target node j with radius $\|\boldsymbol{x}_j - \boldsymbol{z}_{i,j}^{\text{opt}}\|$, it implies that $\text{CRLB}_j(\boldsymbol{z}_{i,j,k}^{\text{opt}}) > \text{CRLB}_j(\boldsymbol{z}_{i,j}^{\text{opt}}) = \text{CRLB}_{i,j} \geq \text{CRLB}_{i,j,k}$, which is again a contradiction. Finally, if $\boldsymbol{z}_{i,j,k}^{\text{opt}}$ is inside the circle centered at target node k with radius d_{thr}, it can be shown via (4.18) that $\text{CRLB}_k(\boldsymbol{z}_{i,j,k}^{\text{opt}}) > \text{CRLB}_{i,j} \geq \text{CRLB}_{i,j,k}$, which leads to a similar contradiction. ■

A.8 Proof of Proposition 8

As $\varepsilon \to 0$, it is almost sure that the points included in the jammer path does not violate the location constraints. The jammer is initially located at the ε-vicinity of $T_{min}^{(0)}$. Since $\varepsilon \to 0$ and assuming that the jammer power is nonzero, the CRLB of $T_{min}^{(0)}$ goes to infinity after initial placement of the jammer. Moreover, since $\varrho > 0$, the target nodes other than $T_{min}^{(0)}$ take finite CRLB values so $T_{min}^{(1)} \neq T_{min}^{(0)}$ unless $N_T = 1$. If $N_T = 1$, the optimal jammer location is on the ε-radius circle around the target node as stated in Proposition 1 so that $\mathbf{z}^{alg} = \mathbf{z}^{(1)}$ is one of the optimal locations for the jammer. If $N_T \geq 2$, iterations begin. The remaining analysis is for the case of $N_T \geq 2$.

Since $\varrho > 0$, there is no point for locating the jammer node such that at that point, the CRLBs of all the target nodes go to infinity. Then, the minimum CRLB in the system is bounded from above with a finite value. Based on the jammer movements during the iterations, the minimum CRLB value is updated; hence, the minimum CRLB values during the iterations can be considered as a

sequence of numbers. By the monotonic sequence property [47], if the minimum CRLB is monotonically increasing during the iterations, since it is bounded from above, it converges to a finite value which can be either a local maxima or the global maxima of the minimum CRLB of the target nodes as a function of the jammer location. If this function is unimodal, i.e., the condition presented in the proposition holds, then the algorithm converges to the global maxima which corresponds to the optimal jammer location $\mathbf{z}^{opt}$. Suppose that there exists a suboptimal point $\mathbf{z}^{sub}$, which different than $\mathbf{z}^{opt}$, on the jammer path such that if the jammer is placed at $\mathbf{z}^{sub}$, at the next iteration of the algorithm, the minimum CRLB does not increase. Furthermore, the minimum CRLB value obtained when the jammer is located at $\mathbf{z}^{sub}$ is strictly less than the max-min CRLB obtained at $\mathbf{z}^{opt}$.

When the jammer node is located at $\mathbf{z}^{sub}$, the number of target nodes with the minimum CRLB can either be 1 or greater than 1. Before proceeding to analyze these cases separately, it is stated that by moving the jammer node by any amount of distance towards any direction in the convex hull formed by the locations of N target nodes ($2 \leq N \leq N_T$), the jammer node cannot get closer to all the N target nodes. Likewise, it is not possible to increase all of the pairwise distances between the jammer node and the N target nodes. Let the number of target nodes with the minimum CRLB be equal to N when the jammer is located at $\mathbf{z}^{sub}$ at the kth iteration of the algorithm. To clarify the statement, let P_1 and P_2 be two different points in the convex hull, i.e., $P_1, P_2 \in Conv(S^{(k)})$ and $P_1 \neq P_2$. Suppose that the jammer node is moved from P_1 to P_2 along the straight line segment between P_1 and P_2. Since the line segment is in the convex hull, there exists at least one vertex of the convex hull which is closer to P_1 compared to P_2 and there also exists at least one vertex which is closer to P_2 compared to P_1. Since the vertices of the convex hull correspond to the locations of some of the N target nodes which form the convex hull, it is not possible to increase or decrease all of the pairwise distances between the jammer and the N target nodes by moving the jammer node from a point to any other point in the convex hull. Since the CRLB of a target node is inversely proportional to the distance between the jammer node and the target node, it is not possible to increase or

decrease the CRLBs of all the target nodes that form the convex hull. Thus, the CRLB of at least one of the target nodes increases and the CRLB of at least one of them decreases as a result of any jammer movement in the convex hull. This also implies that there exists at most one point in the convex hull such that if the jammer node is located at that point, the CRLBs of all the target nodes which form the convex hull are equal to each other (any amount of deviation from that point breaks the equality of the CRLBs).

If the number of target nodes with the minimum CRLB is equal to 1 when the jammer is located at $\mathbf{z}^{sub}$ at the kth iteration of the algorithm, the CRLBs of all other target nodes in the system are strictly greater than $CRLB_{min}^{(k)}$. Let the target node with the minimum CRLB at the kth iteration of the algorithm be target node j. Then, $CRLB_{min}^{(k)} = CRLB_j^{(k)} < CRLB_i^{(k)},\ \forall\, i \in \{1, \ldots, N_T\} \setminus j$. Then, at the $(k+1)$th iteration of the algorithm, the jammer node moves one step size towards target node j. Then, the distance between the jammer node and target node j decreases; hence, $CRLB_j^{(k+1)} > CRLB_j^{(k)}$. Since the jammer node moves in the convex hull formed by the locations of all the target nodes, the CRLB of at least one of the target nodes in the system decreases as a result of the jammer movement. The CRLB is a continuous function of the distance between the jammer node and the target node for all target nodes; hence, there exists a nonzero step size $\rho^{(k)}$ such that if $\delta \leq \rho^{(k)}$, $CRLB_j^{(k+1)} \leq CRLB_i^{(k+1)},\ \forall\, i \in \{1, \ldots, N_T\} \setminus j$. Then, $CRLB_{min}^{(k+1)} = CRLB_j^{(k+1)}$. This implies that $CRLB_{min}^{(k+1)} > CRLB_{min}^{(k)}$. Since $\delta \to 0$, by choosing δ to be less than the the minimum of the sequence of $\rho^{(k)}$'s for all k, the inequality $\delta \leq \rho^{(k)}$ can always be satisfied. Therefore, if the number of target nodes with the minimum CRLB at an iteration is 1, then at the next iteration, the minimum CRLB value increases. Therefore, there cannot exist a suboptimal point at which if the jammer node is located, only one of the target nodes has the minimum CRLB.

If the number of target nodes with the minimum CRLB is equal to N ($2 \leq N \leq N_T$) when the jammer node is located at $\mathbf{z}^{sub}$ at the kth iteration of the algorithm, it is either $\mathbf{z}^{sub} \notin Conv(S^{(k)})$ or $\mathbf{z}^{sub} \in Conv(S^{(k)})$. If $\mathbf{z}^{sub} \notin Conv(S^{(k)})$, then at the next iteration of the algorithm, the jammer moves towards its projection onto $Conv(S^{(k)})$ so that the CRLBs of all N target nodes increase. Based on similar

arguments to those in the previous paragraph, the minimum CRLB in the system increases at the next iteration of the algorithm. Therefore, there cannot exist a suboptimal point at which if the jammer node is located, the CRLBs of at least two target nodes are equal to each other and the suboptimal point is outside the convex hull formed by the locations of the target nodes with the minimum CRLB. If $\mathbf{z}^{sub} \in Conv(S^{(k)})$, then at the next iteration of the algorithm, the jammer node moves towards one of the target nodes with the minimum CRLB. Since the jammer moves in the convex hull formed by the target nodes with the minimum CRLB, it is certain that the CRLB of at least one of these target nodes increases and CRLB of at least one of them decreases. Thus, if such a suboptimal point exists, then at the next iteration, the minimum CRLB value decreases. Therefore, it must be shown that there cannot exist such a $\mathbf{z}^{sub}$.

It is stated in Proposition 7 that under the absence of location constraints for the jammer node, the optimal jammer location is determined by at most three target nodes in the system and the CRLBs of at least two target nodes are equal to each other and to the minimum CRLB in the system, when the jammer node is placed at the optimal location. The optimal location for the jammer node lies in the convex hull (triangle) formed by the three target nodes. Based on this fact, let target nodes m, n, and k determine the optimal jammer location so that $CRLB_{min} = CRLB_m(\mathbf{z}^{opt}) = CRLB_n(\mathbf{z}^{opt}) = CRLB_k(\mathbf{z}^{opt}) \leq CRLB_i(\mathbf{z}^{opt}),\ \forall\, i \in \{1, \ldots, N_T\} \setminus \{m, n, k\}$, where $CRLB_m(\mathbf{z}^{opt})$ represents the CRLB of target node m when the jammer node is located at $\mathbf{z}^{opt}$. Since $\mathbf{z}^{sub} \neq \mathbf{z}^{opt}$, when the jammer node is located at $\mathbf{z}^{sub}$, at least one of the target nodes among m, n, and k takes a lower CRLB value compared to its CRLB when the jammer node is located at $\mathbf{z}^{opt}$. Assume, without loss of generality, that target node m takes a lower value, i.e., $CRLB_m(\mathbf{z}^{sub}) < CRLB_m(\mathbf{z}^{opt})$. Furthermore, since $\mathbf{z}^{sub} \in Conv(S^{(k)})$ and the CRLBs of the N target nodes which form $Conv(S^{(k)})$ are equal to each other and to the minimum CRLB in the system, when the jammer node is located at $\mathbf{z}^{opt}$, at least one of the N target nodes gets a lower CRLB compared to its CRLB when the jammer node is located at $\mathbf{z}^{sub}$. Let this target node be target node b so that $CRLB_b(\mathbf{z}^{opt}) < CRLB_b(\mathbf{z}^{sub})$. Moreover, by the definition of the optimal point, $CRLB_m(\mathbf{z}^{opt}) \leq CRLB_b(\mathbf{z}^{opt})$. If all the

inequalities are combined, it is observed that $CRLB_m(\mathbf{z}^{sub}) < CRLB_m(\mathbf{z}^{opt}) \leq CRLB_b(\mathbf{z}^{opt}) < CRLB_b(\mathbf{z}^{sub})$. Initially, it was assumed that when the jammer node is located at $\mathbf{z}^{sub}$, the CRLBs of the N target nodes which form $Conv(S^{(k)})$ are equal to the minimum CRLB in the system. However, it is shown that there exists at least one target node (target node m) with a lower CRLB value than the CRLB of the N target nodes, which leads to a contradiction. Therefore, there cannot exist such a suboptimal point. Note that same arguments apply if the CRLBs of only two target nodes are equal to each other at the optimal jammer location (e.g., $CRLB_{min} = CRLB_m(\mathbf{z}^{opt}) = CRLB_n(\mathbf{z}^{opt}) \leq CRLB_i(\mathbf{z}^{opt}),\ \forall\, i \in \{1, \ldots, N_T\} \setminus \{m, n\}$).

Therefore, no suboptimal points can exist on the jammer path and the minimum CRLB monotonically increases during the iterations of the algorithm. Then, the jammer location determined in the algorithm converges almost surely to the optimal jammer location at which the minimum CRLB is maximized. ■